Electronic Research Archive

https://www.aimspress.com/journal/era

ERA, 33(4): 1998–2031.
DOI: 10.3934/era.2025089
Received: 16 December 2024
Revised: 26 March 2025
Accepted: 29 March 2025
Published: 09 April 2025

Research article

The Ill-posedness and Fourier regularization for the backward heat conduction equation with uncertainty

Hong Yang*and Yiliang He

College of Mathematics and Statistics, Northwest Normal University, Lanzhou 730070, China

* **Correspondence:** Email: ysin888@163.com; Tel: +86 13619316908.

Abstract: The backward heat conduction problem (BHCP) is an important branch of inverse problems in mathematical physics. It is widely used and is one of the hot research fields nowadays. However, due to the ill-posedness of the inverse problem, the solution of the problem is difficult to obtain. Therefore, it is necessary to study regularization methods to solve such problems. This paper introduces the backward heat conduction equation (BHCE) with uncertainty and investigates its numerical solution. The uncertainty of parameters in the system is modeled by a fuzzy number. In the solution process, it is first proved that the equation is seriously ill-posed under the concept of granular differentiability. Second, a Fourier regularization method based on the fuzzy Fourier transform is proposed to solve the BHCE with uncertainty, and the granular representation of the approximate solution is given. Finally, some error estimates between the approximate solution and exact solution are provided under the condition of the prior bound assumptions and suitable choices of regularization parameters. Numerical examples also demonstrate the effectiveness and practicability of the proposed method.

Keywords: fuzzy numbers; ill-posedness; granular differentiability; Fourier regularization; fuzzy Fourier transform; error estimate

1. Introduction

In recent years, the inverse problem has aroused the research interest of scholars. Keller first proposed the concept of positive and inverse problems in [1]. Solving problems based on known data and definite solution conditions is called a positive problem (also known as a direct problem). On the contrary, problems like those of interest in this paper are called inverse problems if we solve or estimate unknown data based on measurement data. Hadamard [2] first proposed the concept of well-posedness. That is, a problem is well-posed if its solution exists and is unique and stable to the given data. If one of these is not satisfied, then the problem is ill-posed. With the study of the inverse problem, people find that the inverse problem is usually ill-posed. So, studying the solution of the inverse problem is

a challenging task. The heat conduction equation is a classical mathematical physics equation, which describes the process of temperature change with time in a certain region. If we already know the initial temperature and boundary conditions of the equation, and we obtain the temperature at any time by solving the equation, this is called the forward heat conduction problem, and the forward problem is well-posed in general. In real life, since the initial temperature in the heat equation is unknown, then we have to use some conditions to obtain the initial temperature and the temperature distribution at any time. This kind of problem is called the backward heat conduction problem. For example, in the field of biomedicine, through changes in the body's perceived temperature, we can determine that a disease is occurring in one of the body's organs [3–5]. The BHCP is also called the final value problem [6], which is a seriously ill-posed problem [7]. Usually, there is no solution, or if there is a solution, it will be discontinuously dependent on the given data. So, it is very difficult to get its numerical solution. A specific method (called the regularization method) is required to obtain stable numerical solutions. For this reason, many scholars have done a lot of research.

The Tikhonov regularization method to solve the BHCE by W. B. Muniz et al. was proposed in [8, 9]. The author transforms this inverse problem into an optimization problem. The regular term is introduced into the objective function, and a good approximation is obtained. In [10], in order to solve the inverse heat equation, the author proposes a new Tikhonov method. In [11], the Lie-group shooting method is used to numerically integrate the ordinary differential equations. S. M. Kirkup and M. Wadsworth proposed operator splitting in [12] and obtained the solution of the inverse heat equation. The Adomian decomposition method was proposed by G. Adomian, R. Grzymkowski, and M. Pleszczynski in [13, 14]. In [15], a new spatiotemporal radial Trefftz collocation method was proposed to solve the inverse heat conduction problem with time-dependent source terms.

In recent years, the Fourier regularization method has been found to be highly efficient in solving inverse problems. In [16, 17], Fourier regularization was applied to study the heat equation. In [18], the author studied numerical differentiation. In [19], a posterior truncation method was proposed to solve ill-posed problems. In [20,21], the author solved the Cauchy problem of Helmholtz equation by a truncation method. In [22], the authors studied the Cauchy problem of the inhomogeneous Helmholtz equation. In [23], the initial data of the BHCP with non-uniform time fraction was determined by the Fourier truncation method. In [24], a new technique for determining the truncation singular value when regularization is applied in ill-posed inverse problems is discussed. Besides, the Fourier-type inversion has been characterized in a general setting of the filter regularization operators in [25]. Other methods for solving the inverse problem of heat conduction can be found in references [26–30].

Although the authors in the above literature have obtained the solution of the BHCE through some regularization methods, the error estimation is basically the traditional *Hölder* type estimation, and the estimation at $t = 0$ is neglected. In addition, the traditional heat conduction equation does not take into account the uncertainty of the parameters and regards the parameters as definite values, which is a big defect when we solve real-world problems. For example, in the process of the spacecraft returning to the land surface, due to the effect of aerodynamic heating of the atmosphere, the temperature of the spacecraft surface rises instantaneously with the passage of time. Therefore, we must get the surface temperature in time to ensure the safety of the astronauts. But, this temperature is often difficult to measure, and when it is measured, it is uncertain. For instance, in the high-temperature smelting furnace in the high-temperature smelting operation, we need to regularly measure the temperature of the furnace surface to ensure safety. However, due to the extremely high temperature of the furnace

surface, the data measured by physical means are often uncertain. In order to deal with the uncertainty in parameters, we use fuzzy numbers to model the uncertainty in parameters and define the BHCE with uncertainty. Since the BHCE with uncertainty is a fuzzy differential equation in essence, some literature on fuzzy differential equations is introduced here for the convenience of analysis.

The theories related to fuzzy differential equations have been extensively studied, but because of the operation property of fuzzy subtraction, it is very difficult to define the derivative of fuzzy numbers, which is a great challenge. The development of derivatives of fuzzy numbers is described below.

In 1965, Zadeh proposed the concept of fuzzy sets for the first time in [31]. The fuzzy mapping function was introduced by Chang and Zadeh in [32]. In 1972, under the influence of the extension principle, Dubois et al. [33] proposed elementary fuzzy operation. The cauchy problem for fuzzy differential equations (FDEs) were studied by Kaleva in [34]. The fuzzy initial value problem was studied by Seikkala in [35]. Based on the Hukuhara derivative operation, Bade applied it to the solution of FDEs in [36]. A differential transform method to solve fuzzy partial differential equations (FPDEs) was studied by Mikaeilvand and Khakrangin in [37]. Zadeh's extension principle was applied to the solution of FDEs by M. S. Cecconello, M. Oberguggenberger et al. in [38, 39]. S. Abbasbandy and M. Chen proposed solving fuzzy differential equations based on differential inclusion theory in [40, 41], which forms a differential inclusion family by taking the level set of fuzzy vector fields. In [42], based on the Hukuhara derivative and the generalized Bede derivative, a fuzzy differential equation was solved by R. Agarwal and M. Chen et al. In 1997, Zadeh put forward the idea of fuzzy information granulation in [43]. In 2018, M. Mazandarani proposed a new method for solving fuzzy differential equations, namely granular differentiability, in [44]. This method overcomes the disadvantages of previous methods and makes the solution of fuzzy differential equations simple and convenient. According to our literature review, the conventional fuzzy differential equation is generally based on the μ-level set of fuzzy numbers into two crisp differential equations to obtain the solution interval. However, in this paper, we use the concept of the granular differentiability to transform the fuzzy differential equation into a granular differential equation, thus improving the efficiency of the calculation.

In this paper, we will regard the parameters in the BHCE as uncertain parameters, and define the BHCE with uncertainty. It is found that most of the papers are on the forward problem of fuzzy differential equations, while there are very few papers on the inverse problem (such as ill-posedness, regularization methods, etc). The representative studies are mainly the following articles by Gong and Yang. In [45], Gong and Yang studied fuzzy initial boundary value problems in 2015. A regularization method was proposed to restore numerical stability. In 2019, Yang and Gong first proposed the concept of ill-posedness of the first kind of the fuzzy Fredholm integral equation in [46]. In [47], Yang and Gong proposed an iterative method for solving the fuzzy integral equation. The error estimation under this method is also given.

The remaining portion of the current paper is arranged as follows. In Section 2, the basic knowledge used in this paper is given. In Section 3, the BHCE with uncertain parameters is defined and the granular representation is derived. Then, it is proved to be a seriously ill-posed equation. In Section 4, the Fourier regularization method is introduced, and the granular representation of the approximate solution is given. Under the condition of proper selection of regularization parameters, the error estimation between approximate solution and exact solution is proved. In Section 5, a numerical example is given to illustrate the feasibility and practicability of the method. Section 6 gives the

conclusion of this paper and future prospects.

2. Preliminaries

We stipulate that the fuzzy number space is represented by E^1. For $0 < \mu \leq 1$, the μ-level set of $\tilde{u} \in E^1$ is defined by $[\tilde{u}]_\mu = \{x \in \mathbb{R}^n | \tilde{u}(x) \geq \mu\}$.

Theorem 2.1. *([48]) If $\tilde{u} \in E^1$, then $\tilde{u} = \bigcup\limits_{\mu\in[0,1]} (\mu \cdot [\tilde{u}]_\mu)$.*

Definition 2.2. *([44]) Let $\tilde{u} : [a, b] \subseteq \mathbb{R}^n \to [0, 1]$ be a fuzzy number. The horizontal membership function $u^{gr} : [0, 1] \times [0, 1] \to [a, b]$ is a representation of $\tilde{u}(x)$ as $u^{gr}(\mu, \alpha_u) = x$ in which "gr" stands for the granule of information included in $x \in [a, b], \mu \in [0, 1]$ is the membership degree of x in $\tilde{u}(x), \alpha_u \in [0, 1]$ is called relative-distance-measure (RDM) variable, and $u^{gr}(\mu, \alpha_u) = \underline{u}^\mu + (\overline{u}^\mu - \underline{u}^\mu)\alpha_u$.*

By definition, for fuzzy numbers $\tilde{u} = (a, b, c)$, we have $\mathcal{H}(\tilde{u}) = [a + (b - a)\mu] + [(1 - \mu)(c - a)]\alpha_u$.

Remark 2.3. *([44]) The horizontal membership function of $\tilde{u}(x) \in E^1$ is also denoted by $\mathcal{H}(\tilde{u}(x)) = u^{gr}(\mu, \alpha_u)$. Moreover, using*

$$\mathcal{H}^{-1}(u^{gr}(\mu, \alpha_u)) = [\tilde{u}]_\mu = \left[\inf_{\beta\geq\mu} \min_{\alpha_u} u^{gr}(\beta, \alpha_u), \sup_{\beta\geq\mu} \max_{\alpha_u} u^{gr}(\beta, \alpha_u)\right], \tag{2.1}$$

the μ-level sets of the vertical membership function of $\tilde{u}(x)$, which is in fact the span of the information granule, can be obtained.

Example 2.4. *For $\tilde{\mu} = (2, 3, 5, 6) \in E^1$,*

$$\tilde{\mu}(x) = \begin{cases} x - 2, & x \in [2, 3), \\ 1, & x \in [3, 5], \\ -x + 6, & x \in (5, 6], \\ 0, & otherwise. \end{cases} \tag{2.2}$$

Figure 1 shows its horizontal membership function.

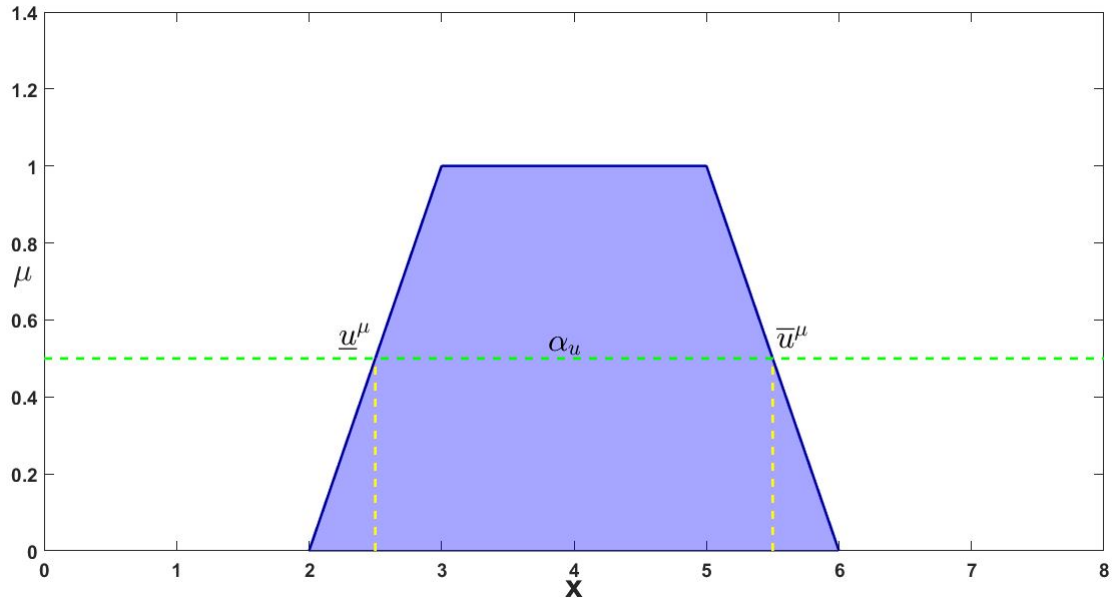

Figure 1. The trapezoidal fuzzy interval number $\tilde{\mu} = (2, 3, 5, 6)$.

Definition 2.5. *([44]) Two fuzzy numbers $\tilde{u}$ and $\tilde{v}$ are said to be equal if and only if $\mathcal{H}(\tilde{u}) = \mathcal{H}(\tilde{v})$ for all $\alpha_u = \alpha_v \in [0, 1]$, and $\mu \in [0, 1]$.*

Definition 2.6. *([44, 49]) Let $\tilde{f} : [a, b] \subseteq \mathbb{R}^n \to E^1$. The horizontal membership function of $\tilde{f}(t)$ at the point $t \in [a, b]$ is denoted by $\mathcal{H}(\tilde{f}(t)) \triangleq f^{gr}(t, \mu, \alpha_f)$, and defined as $f^{gr} : [a, b] \times [0, 1] \times \underbrace{[0, 1] \times \cdots \times [0, 1]}_{n} \to [c, d] \subseteq \mathbb{R}$ in which $\alpha_f \triangleq (\alpha_{u_1}, \alpha_{u_2}, \cdots, \alpha_{u_n})$ are the RDM variables corresponding to the fuzzy numbers.*

Theorem 2.7. *([44]) The fuzzy-number-valued function $\tilde{f} : [a, b] \subseteq \mathbb{R}^n \to E^1$ is said to be gr-differentiable at the point $t \in [a, b]$ if and only if its horizontal membership function is differentiable with respect to t at that point. Moreover, $\mathcal{H}\left(\dfrac{d\tilde{f}(t)}{dt}\right) = \dfrac{\partial f^{gr}(t, \mu, \alpha_f)}{\partial t}$.*

Definition 2.8. *[44] Let $\int_a^b \tilde{f}(t)dt$ denote the integral of $\tilde{f}$ on $[a, b]$. Then, the fuzzy function $\tilde{f}$ is said to be granular integrable on $[a, b]$ if there exists a fuzzy number $\tilde{m} = \int_a^b \tilde{f}(t)dt$ such that $\mathcal{H}(\tilde{m}) = \int_a^b \mathcal{H}(\tilde{f}(t))dt$.*

Definition 2.9. *[44] Let $\tilde{u}$ and $\tilde{v}$ be two fuzzy numbers whose horizontal membership functions are $u^{gr}(\mu, \alpha_u)$ and $v^{gr}(\mu, \alpha_v)$, respectively, and " $\odot_{gr}$ " denotes one of the four basic operations, i.e., addition, subtraction, multiplication, and division. Then, $\tilde{u} \odot_{gr} \tilde{v}$ is a fuzzy number $\tilde{m}$ such that $\mathcal{H}(\tilde{m}) \triangleq u^{gr}(\mu, \alpha_u) \odot_{gr} v^{gr}(\mu, \alpha_v)$.*

Remark 2.10. *[44] Let $\tilde{m} = \tilde{u} \odot_{gr} \tilde{v}$. Then, $[\tilde{m}]_\mu = \mathcal{H}^{-1}(u^{gr}(\mu, \alpha_u) \odot_{gr} v^{gr}(\mu, \alpha_v))$ always presents μ-level sets of the fuzzy number $\tilde{m}$.*

Remark 2.11. *[44] Consider the differential equation*

$$\begin{cases} \dot{\tilde{x}}(t) = \tilde{f}(t, \tilde{x}(t)), \quad t \in [t_0, t_f], \\ \tilde{x}(t_0) = \tilde{x}_0, \end{cases} \tag{2.3}$$

where $\tilde{x} : [t_0, t_f] \subseteq \mathbb{R} \to E^1$ *includes* $n \in \mathbb{N}$ *distinct fuzzy numbers* $\tilde{u}_1, \tilde{u}_2, ..., \tilde{u}_n$, $\dot{\tilde{x}}(t)$ *represents the gr-derivative of* $\tilde{x}$ *with respect to t, and* $\tilde{x}_0 \in E^1$ *is a fuzzy initial condition. Based on Definition* 2.5*, the fuzzy differential Equation* (2.3) *can be rewritten as*

$$\begin{cases} \mathcal{H}(\dot{\tilde{x}}(t)) = \mathcal{H}(\tilde{f}(t, \tilde{x}(t))), \quad t \in [t_0, t_f], \\ \mathcal{H}(\tilde{x}(t_0)) = \mathcal{H}(\tilde{x}_0), \end{cases} \tag{2.4}$$

and then, using Theorem 2.7*, we have*

$$\begin{cases} \dfrac{\partial x^{gr}(t, \mu, \alpha)}{\partial t} = f^{gr}(t, x^{gr}(t, \mu, \alpha), \mu, \alpha), & t \in [t_0, t_f], \\ x^{gr}(t_0, \mu, \alpha) = x_0^{gr}(\mu, \alpha), & \alpha \triangleq (\alpha_{u_1}, \alpha_{u_2}, ..., \alpha_{u_n}). \end{cases} \tag{2.5}$$

Definition 2.12. *Let* $\tilde{f}(t)$ *be a bounded and continuous fuzzy-number-valued function. Then, the fuzzy Fourier transform of* $\tilde{f}(t)$ *is given by the following formula:*

$$\hat{\tilde{f}}(t) := \mathcal{F}\{\tilde{f}(t)\} = \frac{1}{\sqrt{2\pi}} \int_{-\infty}^{+\infty} \tilde{f}(t) e^{-iwt} dt = \tilde{F}(w). \tag{2.6}$$

Definition 2.13. *If* $\tilde{F}(w)$ *is the fuzzy Fourier transform of* $\tilde{f}(t)$*, then the inverse fuzzy Fourier transform of* $\tilde{F}(w)$ *is*

$$\mathcal{F}^{-1}\{\tilde{F}(w)\} = \frac{1}{\sqrt{2\pi}} \int_{-\infty}^{+\infty} \tilde{F}(w) e^{iwt} dw = \tilde{f}(t). \tag{2.7}$$

Remark 2.14. *Let* $\tilde{f}(x)$ *be a fuzzy-number-valued function. According to Definition* 2.8*, for any* $\mu, \alpha_f, \alpha_F \in [0, 1]$*, the following formula holds:*

$$\mathcal{F}\{f^{gr}(t, \mu, \alpha_f)\} = \frac{1}{\sqrt{2\pi}} \int_{-\infty}^{+\infty} f^{gr}(t, \mu, \alpha_f) e^{-iwt} dt = F^{gr}(w, \mu, \alpha_F), \tag{2.8}$$

and Eq (2.7) *can also be rewritten as*

$$\mathcal{F}^{-1}\{F^{gr}(w, \mu, \alpha_F)\} = \frac{1}{\sqrt{2\pi}} \int_{-\infty}^{+\infty} F^{gr}(w, \mu, \alpha_F) e^{iwt} dw = f^{gr}(t, \mu, \alpha_f). \tag{2.9}$$

Example 2.15. *[50] Consider the following fuzzy heat conduction equation:*

$$\begin{cases} \partial_{t_{gr}} \tilde{u}(x, t) \ominus_{gr} k \partial_{x x_{gr}} \tilde{u}(x, t) = 0, \quad t \geq 0, \\ \tilde{u}(x, 0) = \tilde{\varphi}(x), \qquad\qquad x \in \mathbb{R}, \end{cases} \tag{2.10}$$

where $k \in \mathcal{R}$ *represents the coefficient, and* $\tilde{\varphi}(x)$ *is the fuzzy initial condition. If we assume that the exact solution* $\tilde{u}(x, t)$ *of the above equation has a fuzzy Fourier transform of* $\mathcal{F}\{\tilde{u}(x, t)\}$ *with respect to the variable x, then by Definition* 2.12*, we have*

$$\mathcal{F}\{\tilde{u}(x, t)\} = \frac{1}{\sqrt{2\pi}} \int_{-\infty}^{+\infty} e^{-i\lambda x} \tilde{u}(x, t) dx = \tilde{F}(\lambda, t), \tag{2.11}$$

and according to Definition 2.13*, we have*

$$\mathcal{F}^{-1}\{\tilde{F}(\lambda,t)\} = \frac{1}{\sqrt{2\pi}}\int_{-\infty}^{+\infty} e^{i\lambda x}\tilde{F}(\lambda,t)d\lambda = \tilde{u}(x,t). \tag{2.12}$$

We apply the fuzzy Fourier transform to the variable x in Eq (2.10)*, and obtain its exact solution by the variable separation method as follows:*

$$\tilde{F}(\lambda,t) = \tilde{F}(\lambda,0)e^{k\lambda^2 t}, \tag{2.13}$$

where $\tilde{F}(\lambda,0)$ *is the fuzzy Fourier transform of fuzzy initial data* $\tilde{\varphi}(x)$*, i.e.,*

$$\tilde{F}(\lambda,0) = \frac{1}{\sqrt{2\pi}}\int_{-\infty}^{+\infty} e^{-i\lambda x}\tilde{\varphi}(x)dx. \tag{2.14}$$

Then, we substitute $\tilde{F}(\lambda,t)$ *into the Eq* (2.12)*, and obtain*

$$\begin{aligned}\tilde{u}(x,t) &= \frac{1}{\sqrt{2\pi}}\int_{-\infty}^{+\infty} e^{-k\lambda^2 t}e^{i\lambda x}\tilde{F}(\lambda,0)d\lambda \\ &= \frac{1}{\sqrt{2\pi}}\int_{-\infty}^{+\infty}\left(\int_{-\infty}^{+\infty} e^{-i\lambda\zeta}\tilde{\varphi}(\zeta)d\zeta\right)e^{-k\lambda^2 t}e^{i\lambda x}d\lambda \\ &= \frac{1}{\sqrt{2\pi}}\int_{-\infty}^{+\infty}\tilde{\varphi}(\zeta)\int_{-\infty}^{+\infty} e^{-k\lambda^2 t}e^{i\lambda(x-\zeta)}d\lambda d\zeta,\end{aligned} \tag{2.15}$$

where the exponent part can be written as

$$-k\lambda^2 t + i\lambda(x-\zeta) = -tk\left(\lambda^2 - i\lambda\frac{x-\zeta}{kt}\right) = -kt\left[\left(\lambda - i\frac{x-\zeta}{2kt}\right)^2 + \frac{(x-\zeta)^2}{4k^2t^2}\right]. \tag{2.16}$$

Let

$$\begin{aligned}G(x,t,\zeta) &= \int_{-\infty}^{+\infty} e^{-k\lambda^2 t}e^{i\lambda(x-\zeta)}d\lambda \\ &= \int_{-\infty}^{+\infty} e^{\left[-kt\left(\lambda - i\frac{x-\zeta}{2kt}\right)^2 - \frac{(x-\zeta)^2}{4kt}\right]}.\end{aligned} \tag{2.17}$$

If we set $\lambda - i\dfrac{x-\zeta}{2kt} = \dfrac{l}{\sqrt{kt}}$*, then* $d\lambda = \dfrac{1}{\sqrt{kt}}dl$*. According to Euler*′*s equation (denoted as* $\int_{-\infty}^{+\infty} e^{-l^2}dl = \sqrt{\pi}$*), we obtain*

$$G(x,t,\zeta) = \int_{-\infty}^{+\infty} e^{-l}e^{-\left[\frac{(x-\zeta)^2}{kt}\right]}\frac{1}{\sqrt{4kt}} = \sqrt{\frac{\pi}{kt}}e^{-\left[\frac{(x-\zeta)^2}{4kt}\right]}. \tag{2.18}$$

We get the solution of the fuzzy heat conduction equation as follows:

$$\tilde{u}(x,t) = \frac{1}{\sqrt{4\pi kt}}\int_{-\infty}^{+\infty} e^{-\frac{(x-\zeta)^2}{4kt}}\tilde{\varphi}(\zeta)d\zeta, \tag{2.19}$$

and according to Definition 2.8*, we have*

$$u^{gr}(x,t,\mu,\alpha) = \frac{1}{\sqrt{4\pi kt}}\int_{-\infty}^{+\infty} e^{-\frac{(x-\zeta)^2}{4kt}}\varphi^{gr}(\zeta,\mu,\alpha)d\zeta. \tag{2.20}$$

Definition 2.16. *([51]) Let the fuzzy-number-valued function $\tilde{f}(x)$ be granular improper integrable on the infinite interval $[a, \infty)$, where $a \geq 0$. For any fixed $\mu, \alpha \in [0, 1]$, then L^2-norm of $f^{gr}(x, \mu, \alpha)$ on $\mathbb{R}$ is defined as*

$$\mathcal{H}\left(\| \tilde{f}(x) \|_2\right) = \| \mathcal{H}\left(\tilde{f}(x)\right) \|_2 = \left(\int_a^{\infty} (f^{gr}(x, \mu, \alpha))^2 \, dx\right)^{\frac{1}{2}}. \tag{2.21}$$

3. Ill-posedness of the BHCE with uncertainty

In this section, we consider the following BHCE with uncertainty:

$$\begin{cases} \partial_{t_{gr}} \tilde{u}(x, t) \ominus_{gr} \partial_{xx_{gr}} \tilde{u}(x, t) = 0, & -\infty < x < +\infty, 0 \leq t < T, \\ \tilde{u}(x, T) = \tilde{\varphi}_T(x), & -\infty < x < +\infty, \end{cases} \tag{3.1}$$

where $\tilde{\varphi}_T(x)$ is the data known at time T. We want to find the temperature distribution $\tilde{u}(\cdot, t)$ at time $0 \leq t < T$ from the data we know, $\tilde{\varphi}_T(x)$.

According to Remark 2.11, the above Eq (3.1) can be rewritten as

$$\begin{cases} \partial_{t_{gr}} u^{gr}(x, t, \mu, \alpha_u) \ominus_{gr} \partial_{xx_{gr}} u^{gr}(x, t, \mu, \alpha_u) = 0, & x \in \mathbb{R}; t \in [0, T), \\ u^{gr}(x, T, \mu, \alpha_u) = \varphi_T^{gr}(x, \mu, \alpha_\varphi), & \alpha_u = \alpha_\varphi \in [0, 1]. \end{cases} \tag{3.2}$$

Based on the Definition 3.1 below, we will show that the BHCE with uncertainty is seriously ill-posed.

Definition 3.1. *An equation is well-posed if its solution satisfies the following three properties:*
(1) *Existence;*
(2) *Uniqueness;*
(3) *Continuous dependence on given data.*

On the contrary, if only one of these three conditions is not satisfied, then it is ill-posed.

Theorem 3.2. *If Eq* (3.2) *has no solution, then Eq* (3.1) *has no solution.*

Proof. If Eq (3.2) has no solution, for any $\mu, \alpha \in [0, 1]$, then $u^{gr}(x, t, \mu, \alpha)$ does not exist. From Remark 2.3, we can get that $\mathcal{H}^{-1}(u^{gr}(x, t, \mu, \alpha)) = [\tilde{u}(x, t)]_\mu$ does not exist. According to Theorem 2.1, $\tilde{u}(x, t)$ does not exist. Therefore, Equation (3.1) has no solution. □

Theorem 3.3. *If the solution of Eq* (3.2) *exists and it is not unique, then a solution of Eq* (3.1) *exists and it is not unique.*

Proof. For $x \in \mathbb{R}$, $t \in (0, T]$, $\mu, \alpha \in [0, 1]$, assume $u_1^{gr}(x, t, \mu, \alpha_u)$ and $u_2^{gr}(x, t, \mu, \alpha_u)$ are the solution of Eq (3.2) which correspond to the data $\varphi_T^{gr}(x, \mu, \alpha_\varphi)$, respectively, and $u_1^{gr}(x, t, \mu, \alpha_u) \neq u_2^{gr}(x, t, \mu, \alpha_u)$. According to the Eq (3.2), we have the following equation:

$$\begin{cases} \partial_{t_{gr}} u_1^{gr}(x, t, \mu, \alpha_u) \ominus_{gr} \partial_{xx_{gr}} u_1^{gr}(x, t, \mu, \alpha_u) = 0, \\ u_1^{gr}(x, T, \mu, \alpha_u) = \varphi_T^{gr}(x, \mu, \alpha_\varphi), \end{cases} \tag{3.3}$$

$$\begin{cases} \partial_{t_{gr}} u_2^{gr}(x, t, \mu, \alpha_u) \ominus_{gr} \partial_{xx_{gr}} u_2^{gr}(x, t, \mu, \alpha_u) = 0, \\ u_2^{gr}(x, T, \mu, \alpha_u) = \varphi_T^{gr}(x, \mu, \alpha_\varphi). \end{cases} \tag{3.4}$$

For Eq (3.3), we have

$$\begin{cases} \partial_{t_{gr}} u_1^{gr}(x,t,\mu,\alpha_u) = \partial_{xx_{gr}} u_1^{gr}(x,t,\mu,\alpha_u), \\ u_1^{gr}(x,T,\mu,\alpha_u) = \varphi_T^{gr}(x,\mu,\alpha_\varphi). \end{cases} \tag{3.5}$$

For any $\mu, \alpha_u \in [0,1]$, according to Remark 2.11, we have

$$\begin{cases} \mathcal{H}\left(\partial_{t_{gr}} \tilde{u}_1(x,t)\right) = \mathcal{H}\left(\partial_{xx_{gr}} \tilde{u}_1(x,t)\right), \\ \mathcal{H}\left(\tilde{u}_1(x,T)\right) = \mathcal{H}\left(\tilde{\varphi}_T(x)\right). \end{cases} \tag{3.6}$$

For Eq (3.6), we have

$$\begin{cases} \partial_{t_{gr}} \mathcal{H}(\tilde{u}_1(x,t)) = \partial_{xx_{gr}} \mathcal{H}(\tilde{u}_1(x,t)), \\ \mathcal{H}\left(\tilde{u}_1(x,T)\right) = \mathcal{H}\left(\tilde{\varphi}_T(x)\right), \end{cases} \tag{3.7}$$

and, according to Definition 2.5 and Eq (3.7), we have

$$\begin{cases} \partial_{t_{gr}} \tilde{u}_1(x,t) = \partial_{xx_{gr}} \tilde{u}_1(x,t), \\ \tilde{u}_1(x,T) = \tilde{\varphi}_T(x). \end{cases} \tag{3.8}$$

For Eq (3.8), we have

$$\begin{cases} \partial_{t_{gr}} \tilde{u}_1(x,t) \ominus_{gr} \partial_{xx_{gr}} \tilde{u}_1(x,t) = 0, \\ \tilde{u}_1(x,T) = \tilde{\varphi}_T(x). \end{cases} \tag{3.9}$$

In the same way, for Eq (3.4), we can also get the following equations:

$$\begin{cases} \partial_{t_{gr}} \tilde{u}_2(x,t) \ominus_{gr} \partial_{xx_{gr}} \tilde{u}_2(x,t) = 0, \\ \tilde{u}_2(x,T) = \tilde{\varphi}_T(x). \end{cases} \tag{3.10}$$

For any $\mu, \alpha \in [0,1]$, because $u_1^{gr}(x,t,\mu,\alpha_u)$ and $u_2^{gr}(x,t,\mu,\alpha_u)$ are the solutions of Eqs (3.2) which correspond to the data $\varphi_T^{gr}(x,\mu,\alpha_\varphi)$, respectively, and $u_1^{gr}(x,t,\mu,\alpha_u) \neq u_2^{gr}(x,t,\mu,\alpha_u)$, according to Remark 2.3, $\mathcal{H}\left(u_1(x,t,\mu,\alpha)\right) \neq \mathcal{H}\left(u_2(x,t,\mu,\alpha)\right)$. According to Definition 2.5, $\tilde{u}_1(x,t) \neq \tilde{u}_2(x,t)$. From Eqs (3.9) and (3.10), we can obtain that $\tilde{u}_1(x,t)$ and $\tilde{u}_2(x,t)$ are two different solutions of the Eq (3.1). □

Theorem 3.4. *For any α_φ, $\mu \in [0,1]$, a solution of Eq* (3.2) *does not depend continuously on the data $\varphi_T^{gr}(x,\mu,\alpha_\varphi)$.*

Theorem 3.5. *A solution of Eq* (3.1) *does not depend continuously on the data $\tilde{\varphi}_T(x)$.*

Proof. Using the fuzzy Fourier transform to Eq (3.1) with respect to the variable x, we can get the fuzzy Fourier transform $\hat{\tilde{u}}(\xi,t)$ of the exact solution $\tilde{u}(x,t)$ of Eq (3.1)

$$\hat{\tilde{u}}(\xi,t) = e^{\xi^2(T-t)} \hat{\tilde{\varphi}}_T(\xi), \tag{3.11}$$

or equivalently

$$\tilde{u}(x,t) = \frac{1}{\sqrt{2\pi}} \int_{-\infty}^{+\infty} e^{i\xi x} e^{\xi^2(T-t)} \hat{\tilde{\varphi}}_T(\xi) d\xi. \tag{3.12}$$

Moreover, there holds

$$\hat{\tilde{u}}(\xi, 0) = e^{\xi^2 T}\hat{\tilde{\varphi}}_T(\xi), \tag{3.13}$$

or equivalently

$$\tilde{u}(x, 0) = \frac{1}{\sqrt{2\pi}}\int_{-\infty}^{+\infty} e^{i\xi x}e^{\xi^2 T}\hat{\tilde{\varphi}}_T(\xi)d\xi. \tag{3.14}$$

Now we consider Eq (3.12). Assume $\tilde{F} : R \to E^1$ is a fuzzy-number-valued function. Let $\tilde{u}_1(x, t)$ and $\tilde{u}_2(x, t)$ be the solutions of Eq (3.1) which correspond to the data $\tilde{\varphi}_1(x) = \tilde{\varphi}_T(x)$ and $\tilde{\varphi}_2(x) = \tilde{\varphi}_1(x)\oplus_{gr}\epsilon\sin(\omega x)\odot_{gr}\tilde{F}(x)$ (where ϵ is a nonzero constant). Then, we have the following two equations:

$$\tilde{u}_1(x, t) = \frac{1}{\sqrt{2\pi}}\int_{-\infty}^{+\infty} e^{i\xi x}e^{\xi^2 T}\hat{\tilde{\varphi}}_1(\xi)d\xi, \tag{3.15}$$

$$\tilde{u}_2(x, t) = \frac{1}{\sqrt{2\pi}}\int_{-\infty}^{+\infty} e^{i\xi x}e^{\xi^2 T}\hat{\tilde{\varphi}}_2(\xi)d\xi, \tag{3.16}$$

From Eqs (3.15) and (3.16), we have

$$\tilde{u}_2(x, t) = \tilde{u}_1(x, t)\oplus_{gr}\frac{1}{\sqrt{2\pi}}\int_{-\infty}^{+\infty} e^{i\xi x}e^{\xi^2 T}\epsilon\sin(\omega x)\odot_{gr}\tilde{F}(x)d\xi. \tag{3.17}$$

From Eq (3.17), we obtain

$$\tilde{u}_2(x, t)\ominus_{gr}\tilde{u}_1(x, t) = \frac{1}{\sqrt{2\pi}}\int_{-\infty}^{+\infty} e^{i\xi x}e^{\xi^2 T}\epsilon\sin(\omega x)\odot_{gr}\tilde{F}(x)d\xi. \tag{3.18}$$

For any $\mu, \alpha \in [0, 1]$ and Eq (3.18), according to Remark 2.11 and Definition 2.8, we have

$$u_2^{gr}(x, t, \mu, \alpha)\ominus_{gr}u_1^{gr}(x, t, \mu, \alpha) = \frac{1}{\sqrt{2\pi}}\int_{-\infty}^{+\infty} e^{i\xi x}e^{\xi^2 T}\epsilon\sin(\omega x)\cdot F^{gr}(x, \mu, \alpha)d\xi. \tag{3.19}$$

From equation $\tilde{\varphi}_2(x) = \tilde{\varphi}_1(x)\oplus_{gr}\epsilon\sin(\omega x)\odot_{gr}\tilde{F}(x)$, we obtain

$$\tilde{\varphi}_2(x)\ominus_{gr}\tilde{\varphi}_1(x) = \epsilon\sin(\omega x)\odot_{gr}\tilde{F}(x) \tag{3.20}$$

For any $\mu, \alpha \in [0, 1]$ and Eq (3.20), according to Remark 2.11 and Definition 2.8, we have

$$\varphi_2^{gr}(x, \mu, \alpha)\ominus_{gr}\varphi_1^{gr}(x, \mu, \alpha) = \epsilon\sin(\omega x)\cdot F^{gr}(x, \mu, \alpha), \tag{3.21}$$

and according to the Riemann-Lebesgue Lemma, as $\omega \to 0$, we have the equation

$$\begin{aligned}&\left\|\varphi_2^{gr}(x, \mu, \alpha)\ominus_{gr}\varphi_1^{gr}(x, \mu, \alpha)\right\|_2\\ &= |\epsilon|\left\{\left[\frac{1}{\sqrt{2\pi}}\int_{-\infty}^{+\infty}\sin^2(\omega x)\cdot\left[F^{gr}(x, \mu, \alpha)\right]^2 dx\right]\right\}^{\frac{1}{2}} \to 0.\end{aligned} \tag{3.22}$$

However, as $\omega \to 0$,

$$\begin{aligned}&\left\|u_2^{gr}(x, t, \mu, \alpha)\ominus_{gr}u_1^{gr}(x, t, \mu, \alpha)\right\|_2\\ &= |\epsilon|\left\{\frac{1}{2\pi}\int_{-\infty}^{+\infty}\left[\int_{-\infty}^{+\infty} e^{i\xi x}e^{\xi^2 T}\sin(\omega x)\cdot F^{gr}(x, \mu, \alpha)d\xi\right]^2 dx\right\}^{\frac{1}{2}} \nrightarrow 0,\end{aligned} \tag{3.23}$$

where $\|\cdot\|$ denotes the L^2-norm. (See Definition 2.16.)

The theorem has been proved. □

We will give the following example to help understand Theorem 3.5.

Example 3.6. *Consider the following BHCE:*

$$\begin{cases} \partial_{t_{gr}}\tilde{u}(x,t) \ominus_{gr} \partial_{xx_{gr}}\tilde{u}(x,t) = 0, \quad x \in [0,l], t \in [0,T), \\ \tilde{u}(x,T) = \tilde{\varphi}_T(x), \\ \tilde{u}(0,t) = \tilde{u}(l,t) = 0. \end{cases} \tag{3.24}$$

According to Remark 2.11*, we have the following granular differential equation:*

$$\begin{cases} \partial_{t_{gr}}u^{gr}(t,\mu,\alpha_u) \ominus_{gr} \partial_{xx_{gr}}u^{gr}(x,\mu,\alpha_u) = 0, \quad x \in [0,l], t \in [0,T), \\ u^{gr}(x,T,\mu,\alpha_u) = \varphi_T^{gr}(x,\mu,\alpha_\varphi), \\ u^{gr}(0,t,\mu,\alpha_u) = u^{gr}(l,t,\mu,\alpha_u) = 0, \qquad \alpha_u = \alpha_\varphi \in [0,1]. \end{cases} \tag{3.25}$$

Let $\tilde{\varphi}_{T_1}(x) = 0$*. Then, the corresponding granular equation is* $\varphi_{T_1}^{gr}(x,\mu,\alpha_\varphi) = 0$*. It is easy to verify that, at this time, the solution of the above equation is* $u_1^{gr}(x,t,\mu,\alpha_u) = 0$*.*

Let $\tilde{\varphi}_{T_2} = \tilde{m} \cdot \frac{1}{n} sin\frac{n\pi}{l}x$*, where* $\tilde{m}$ *is a fuzzy-number-valued function, i.e.,* $\tilde{m} = (-1,0,1)$*, which has the following expression:*

$$\tilde{m}(t) = \begin{cases} t+1, t \in [-1,0), \\ 1, t = 0, \\ -t+1, t \in (0,1], \\ 0, t \in (-\infty,-1] \cup [1,+\infty). \end{cases} \tag{3.26}$$

Then, according to Definition 2.6*, we obtain* $m^{gr}(\mu,\alpha_m) = -1+\mu+2(1-\mu)\alpha_m$*. Therefore, the corresponding granular equation is* $\varphi_{T_2}^{gr}(x,\mu,\alpha_\varphi) = [-1+\mu+2(1-\mu)\alpha_m] \cdot \frac{1}{n} sin\frac{n\pi}{l}x$*, for all* $\mu, \alpha_m \in [0.1]$*. In this case, Equation* (3.25) *corresponding to the data* $\varphi_{T_2}^{gr}(x,\mu,\alpha_\varphi)$ *can be solved by the following granular equation:*

$$\begin{cases} u_t^{gr}(t,\mu,\alpha_u) \ominus_{gr} u_{xx}^{gr}(x,u,\alpha_u) = 0, \qquad x \in [0,l], t \in [0,T), \\ u^{gr}(x,T,\mu,\alpha_m) = [-1+\mu+2(1-\mu)\alpha_m] \cdot \frac{1}{n} sin\frac{n\pi}{l}x, \\ u^{gr}(0,t,\mu,\alpha_u) = u^{gr}(l,t,\mu,\alpha_u) = 0, \qquad \alpha_u = \alpha_m \in [0,1]. \end{cases} \tag{3.27}$$

The solution of the above granular differential equation can be easily obtained by the method of separating variables as follows

$$u_2^{gr}(x,t,\mu,\alpha_m) = [-1+\mu+2(1-\mu)\alpha_m]e^{(\frac{n\pi x}{l})^2(T-t)} sin\frac{n\pi}{l}x. \tag{3.28}$$

Based on the above discussion, the continuous dependence of the solution on the given data is analyzed, and we have

$$\sup_{x\in\mathbb{R}} \left|\varphi_{T_1}^{gr}(x,\mu,\alpha_\varphi) \ominus_{gr} \varphi_{T_2}^{gr}(x,\mu,\alpha_\varphi)\right| = \frac{1}{n}[-1+\mu+2(1-\mu)\alpha_m] \to 0, n \to +\infty. \tag{3.29}$$

However, for any $\mu, \alpha_m \in [0,1]$,

$$\sup_{x\in\mathbb{R}} |u_1^{gr}(x,t,\mu,\alpha_u) \ominus_{gr} u_2^{gr}(x,t,\mu,\alpha_m)| = e^{(\frac{n\pi x}{l})^2(T-t)}[-1+\mu+2(1-\mu)\alpha_m] \nrightarrow 0, n \to +\infty. \tag{3.30}$$

Therefore, from Eqs (3.29) *and* (3.30)*, we can conclude that Eq* (3.22) *is seriously ill-posed.*

4. Fourier regularization and error estimates for the BHCE with uncertainty

We consider the BHCE with uncertainty

$$\begin{cases} \partial_{t_{gr}}\tilde{u}(x,t) \ominus_{gr} \partial_{xx_{gr}}\tilde{u}(x,t) = 0, & -\infty < x < +\infty, 0 \le t < T, \\ \tilde{u}(x,T) = \tilde{\varphi}_T(x), & -\infty < x < +\infty, \end{cases} \tag{4.1}$$

where $\tilde{\varphi}_T(x)$ is the data known at time T.

Based on Theorems 3.4 and 3.5, we mainly consider the Fourier regularization of the granular differential equation of the BHCE with uncertainty:

$$\begin{cases} \partial_{t_{gr}}u^{gr}(x,t,\mu,\alpha_u) \ominus_{gr} \partial_{xx_{gr}}u^{gr}(x,t,\mu,\alpha_u) = 0, & x \in \mathbb{R}; t \in [0,T), \\ u^{gr}(x,T,\mu,\alpha_u) = \varphi_T^{gr}(x,\mu,\alpha_\varphi), & \alpha_u = \alpha_\varphi \in [0,1]. \end{cases} \tag{4.2}$$

We need to determine the temperature distribution $u^{gr}(x,t,\mu,\alpha_u)$ for $0 \le t < T$ from the given data $\varphi_T^{gr}(x,\mu,\alpha_\varphi)$. Applying the fuzzy Fourier transform method to Eq (4.2), we can obtain the fuzzy Fourier transform $\hat{u}^{gr}(x,t,\mu,\alpha_u)$ of the solution $u^{gr}(x,t,\mu,\alpha_u)$ of Eq (4.2) as follows:

$$\hat{u}^{gr}(\lambda,t,\mu,\alpha_u) = \mathcal{F}\{u^{gr}(x,t,\mu,\alpha_u)\} = e^{\lambda^2(T-t)}\hat{\varphi}_T^{gr}(\lambda,\mu,\alpha_\varphi), \tag{4.3}$$

and, according to the Definition 2.9 and Remark 2.10, we can obtained the inverse fuzzy Fourier transform of $\hat{u}^{gr}(\lambda,t,\mu,\alpha_u)$:

$$u^{gr}(x,t,\mu,\alpha_u) = \frac{1}{\sqrt{2\pi}}\int_{-\infty}^{+\infty} e^{i\lambda x}e^{\lambda^2(T-t)}\hat{\varphi}_T^{gr}(\lambda,\mu,\alpha_\varphi)d\lambda, \tag{4.4}$$

where $\hat{\varphi}_T^{gr}(\lambda,\mu,\alpha_\varphi)$ is the fuzzy Fourier transform of the given data $\varphi_T^{gr}(x,\mu,\alpha_\varphi)$.

For Eq (4.3), let $t = 0$. Then, we have

$$\hat{u}^{gr}(\lambda,0,\mu,\alpha_u) = e^{\lambda^2 T}\hat{\varphi}_T^{gr}(\lambda,\mu,\alpha_\varphi). \tag{4.5}$$

Denoting $u^{gr}(x,0,\mu,\alpha_u) = \varphi_0^{gr}(x,\mu,\alpha_\varphi)$, in order to give an error, we make the following assumption:

$$\| \varphi_0^{gr}(x,\mu,\alpha_\varphi) \|_{H^k} = \| u^{gr}(x,0,\mu,\alpha_u) \|_{H^k} \le A, \tag{4.6}$$

where A represents a positive constant, and $\|\cdot\|_{H^k}$ represents the Sobolev norm.

Based on Eq (4.5), Eq (4.6), and the Parseval identity, we have

$$\| \varphi_0^{gr}(x,\mu,\alpha_\varphi) \|^2 = \int_{-\infty}^{+\infty} |e^{\lambda^2 T}\hat{\varphi}_T^{gr}(\lambda,\mu,\alpha_\varphi)|^2 d\lambda < \infty. \tag{4.7}$$

We find that $e^{\lambda^2 T} \to \infty$ when $|\lambda| \to \infty$, so Eq (4.6) implies a rapid decay of $\hat{\varphi}_T^{gr}(\lambda, \mu, \alpha_\varphi)$ at high frequencies. Since the data $\varphi_{\delta,T}^{gr}(x, t, \mu, \alpha_\varphi)$ at time $t = T$ is measured by a physical instrument, there is a certain error. We know that the ill-posedness of the BHCE with uncertainty is caused by the high-frequency disturbance in the solution. Therefore, in this paper, we apply the Fourier regularization method to stabilize the numerical solution, and instead consider Eq (4.4) only for $|\lambda| < \lambda_{max}$, where λ_{max} is an appropriate positive constant which will be selected as a regularization parameter so that the solution tends to be stable for given noisy data.

Let $\varphi_T^{gr}(x, t, \mu, \alpha_{u\varphi})$ and $\varphi_{\delta,T}^{gr}(x, t, \mu, \alpha_\varphi)$ denote the exact data and measured data at $t = T$, respectively, and they satisfy

$$\| \varphi_T^{gr}(x, t, \mu, \alpha_\varphi) \ominus_{gr} \varphi_{\delta,T}^{gr}(x, t, \mu, \alpha_\varphi) \| \leq \delta, \tag{4.8}$$

where δ denotes the error level, and we assume Eq (4.6) holds.

Next, we define a regularization solution of Eq (4.2) for the measured noisy data, which we call the Fourier regular solution of Eq (4.2) as follows:

$$u_{\delta,\lambda_{\max}}^{gr}(x, t, \mu, \alpha_u) = \frac{1}{\sqrt{2\pi}} \int_{-\infty}^{+\infty} e^{i\lambda x} e^{\lambda^2 (T-t)} \hat{\varphi}_{\delta,T}^{gr}(\lambda, t, \mu, \alpha_\varphi) \zeta_{\max} d\lambda, \tag{4.9}$$

where $\hat{\varphi}_{\delta,T}^{gr}(\lambda, \mu, \alpha_\varphi)$ is the fuzzy Fourier transform of measured the data $\tilde{\varphi}_{\delta,T}(x, t)$ at $t = T$, and $\zeta_{\max}$ is the characteristic function of the interval $[-\lambda_{\max}, \lambda_{\max}]$, i.e.,

$$\zeta_{\max} = \begin{cases} 1, & x \in [-\lambda_{\max}, \lambda_{\max}]; \\ 0, & x \notin [-\lambda_{\max}, \lambda_{\max}], \end{cases} \tag{4.10}$$

and $\lambda_{\max}$ will be selected appropriately as a regularization parameter.

The following theorem illustrates that the Fourier regular solution defined by Eq (4.9) continuously depends on the given data $\varphi_{\delta,T}^{gr}(x, t, \mu, \alpha_\varphi)$.

Theorem 4.1. *Let $u_{\lambda_{\max}}^{gr}(x, t, \mu, \alpha_u)$ and $u_{\delta,\lambda_{\max}}^{gr}(x, t, \mu, \alpha_u)$ be solutions to Eq* (4.9) *corresponding to the data $\varphi_T^{gr}(x, t, \mu, \alpha_\varphi)$ and $\varphi_{\delta,T}^{gr}(x, t, \mu, \alpha_\varphi)$, respectively. Then, for $0 \leq t < T$, there is*

$$\| u_{\lambda_{\max}}^{gr}(\cdot, t, \mu, \alpha_u) \ominus_{gr} u_{\delta,\lambda_{\max}}^{gr}(\cdot, t, \mu, \alpha_u) \| \leq e^{\lambda_{\max}^2 (T-t)} \| \varphi^{gr}(x, t, \mu, \alpha_\varphi) \ominus_{gr} \varphi_\delta^{gr}(x, t, \mu, \alpha_\varphi) \| . \tag{4.11}$$

Proof. Due to the Parseval formula

$$\begin{aligned}
&\| u_{\lambda_{\max}}^{gr}(\cdot, t, \mu, \alpha_u) \ominus_{gr} u_{\delta,\lambda_{\max}}^{gr}(\cdot, t, \mu, \alpha_u) \|^2 \\
=&\| \hat{u}_{\lambda_{\max}}^{gr}(\cdot, t, \mu, \alpha_u) \ominus_{gr} \hat{u}_{\delta,\lambda_{\max}}^{gr}(\cdot, t, \mu, \alpha_u) \|^2 \\
=& \int_{-\infty}^{+\infty} \left| \left[e^{\lambda^2 (T-t)} \left(\hat{\varphi}_T^{gr}(\lambda, \mu, \alpha_\varphi) \ominus_{gr} \hat{\varphi}_{\delta,T}^{gr}(\lambda, \mu, \alpha_\varphi) \right) \right] \right|^2 d\lambda \\
=& \int_{-\lambda_{\max}}^{\lambda_{\max}} \left| \left[e^{\lambda^2 (T-t)} \left(\hat{\varphi}_T^{gr}(\lambda, \mu, \alpha_\varphi) \ominus_{gr} \hat{\varphi}_{\delta,T}^{gr}(\lambda, \mu, \alpha_\varphi) \right) \right] \right|^2 d\lambda \\
\leq& e^{2\lambda_{\max}^2 (T-t)} \int_{-\infty}^{+\infty} \left| \left(\hat{\varphi}_T^{gr}(\lambda, \mu, \alpha_\varphi) \ominus_{gr} \hat{\varphi}_{\delta,T}^{gr}(\lambda, \mu, \alpha_\varphi) \right) \right|^2 d\lambda \\
\leq& e^{2\lambda_{\max}^2 (T-t)} \| \hat{\varphi}_T^{gr}(\lambda, \mu, \alpha_\varphi) \ominus_{gr} \hat{\varphi}_{\delta,T}^{gr}(\lambda, \mu, \alpha_\varphi) \|^2 \\
=\leq& e^{2\lambda_{\max}^2 (T-t)} \cdot \delta^2,
\end{aligned}$$

we have

$$\| u^{gr}_{\lambda_{\max}}(\cdot,t,\mu,\alpha_u) \ominus_{gr} u^{gr}_{\delta,\lambda_{\max}}(\cdot,t,\mu,\alpha_u) \| \leq e^{\lambda^2_{\max}(T-t)} \cdot \delta. \tag{4.12}$$

Therefore, the proof of convergence estimate is completed. □

This theorem shows the stability of the Fourier regularization method. When the input data is noisy, the results indicate that the regularized solution can stay within a reasonable and relatively stable range and will not deviate significantly from the original solution. Thus, it can ensure the reliability and effectiveness of the solution in practical applications.

Note that $\| u^{gr}_{\lambda_{\max}}(\cdot,t,\mu,\alpha_u) \ominus_{gr} u^{gr}_{\delta,\lambda_{\max}}(\cdot,t,\mu,\alpha_u) \| \to 0$ as $\delta \to 0$. That is, the Fourier regular solution defined by Eq (4.9) continuously depends on the given data $\varphi^{gr}_{\delta,T}(x,t,\mu,\alpha_\varphi)$.

Theorem 4.2. *Let $u^{gr}(x,t,\mu,\alpha_u)$ and $u^{gr}_{\delta,\lambda_{\max}}(x,t,\mu,\alpha_u)$ be the exact solution and the Fourier regular solution we defined for the Eq* (4.2)*, respectively. Then, for $0 \leq t \leq T$, assuming that conditions* (4.6) *and Eq* (4.8) *hold, if we select the regularization parameter*

$$\lambda_{\max} = \left(\ln \left(\left(\frac{A}{\delta} \right)^{\frac{1}{T}} \left(\ln \frac{A}{\delta} \right)^{-\frac{k}{2T}} \right) \right)^{\frac{1}{2}}, \tag{4.13}$$

we have the following conclusion:

$$\| u^{gr}(\cdot) \ominus_{gr} u^{gr}_{\delta,\lambda_{\max}}(\cdot) \| \leq A^{1-\frac{t}{T}} \delta^{\frac{t}{T}} (\ln \tfrac{A}{\delta})^{-\frac{k}{2}} \left(1 + \left(\frac{\ln \frac{A}{\delta}}{\frac{1}{T} \ln \frac{A}{\delta} + \ln(\ln \frac{A}{\delta})^{-\frac{k}{2T}}} \right)^{\frac{k}{2}} \right). \tag{4.14}$$

Proof. Due to the Parseval formula and Eqs (4.3)–(4.5), (4.7), and (4.8), we find

$$\begin{aligned}
&\| u^{gr}(\cdot,t,\mu,\alpha_u) \ominus_{gr} u^{gr}_{\delta,\lambda_{\max}}(\cdot,t,\mu,\alpha_u) \| \\
=&\| \hat{u}(\cdot,t,\mu,\alpha_u) \ominus_{gr} \hat{u}^{gr}_{\delta,\lambda_{\max}}(\cdot,t,\mu,\alpha_u) \| \\
=&\| e^{\lambda^2(T-t)} \hat{\varphi}^{gr}_T(\lambda,\mu,\alpha_\varphi) \ominus_{gr} e^{\lambda^2(T-t)} \hat{\varphi}^{gr}_{\delta,T}(\lambda,\mu,\alpha_\varphi) \zeta_{\max} \| \\
=&\| e^{\lambda^2(T-t)} \hat{\varphi}^{gr}_T(\lambda,\mu,\alpha_\varphi) \ominus_{gr} e^{\lambda^2(T-t)} \hat{\varphi}^{gr}_{\delta,T}(\lambda,\mu,\alpha_\varphi) \zeta_{\max} \\
&\oplus_{gr} e^{\lambda^2(T-t)} \hat{\varphi}^{gr}_T(\lambda,\mu,\alpha_\varphi) \zeta_{\max} \ominus_{gr} e^{\lambda^2(T-t)} \hat{\varphi}^{gr}_T(\lambda,\mu,\alpha_\varphi) \zeta_{\max} \| \\
\leq&\| e^{\lambda^2(T-t)} \hat{\varphi}^{gr}_T(\lambda,\mu,\alpha_\varphi) \ominus_{gr} e^{\lambda^2(T-t)} \hat{\varphi}^{gr}_T(\lambda,\mu,\alpha_\varphi) \zeta_{\max} \| \\
&\oplus_{gr} \| e^{\lambda^2(T-t)} \hat{\varphi}^{gr}_T(\lambda,\mu,\alpha_\varphi) \zeta_{\max} \ominus_{gr} e^{\lambda^2(T-t)} \hat{\varphi}^{gr}_{\delta,T}(\lambda,\mu,\alpha_\varphi) \zeta_{\max} \| \\
=&\left(\int_{|\lambda|>\lambda_{\max}} \left| e^{\lambda^2(T-t)} \hat{\varphi}^{gr}_T(\lambda,\mu,\alpha_\varphi) \right|^2 d\lambda \right)^{\frac{1}{2}} \\
&\oplus_{gr} \left(\int_{|\lambda|\leq\lambda_{\max}} \left| e^{\lambda^2(T-t)} \left(\hat{\varphi}^{gr}_{\delta,T}(\lambda,\mu,\alpha_\varphi) \ominus_{gr} \hat{\varphi}^{gr}_T(\lambda,\mu,\alpha_\varphi) \right) \right|^2 d\lambda \right)^{\frac{1}{2}} \\
=&\left(\int_{|\lambda|>\lambda_{\max}} \left| e^{\lambda^2(T-t)} e^{-\lambda^2 T} \hat{\varphi}^{gr}_0(\lambda,\mu,\alpha_\varphi) \right|^2 d\lambda \right)^{\frac{1}{2}}
\end{aligned}$$

$$
\begin{aligned}
&\oplus_{gr}\left(\int_{|\lambda|\le\lambda_{\max}}\left|e^{\lambda^2(T-t)}\left(\hat{\varphi}^{gr}_{\delta,T}(\lambda,\mu,\alpha_\varphi)\ominus_{gr}\hat{\varphi}^{gr}_{T}(\lambda,\mu,\alpha_\varphi)\right)\right|^2 d\lambda\right)^{\frac{1}{2}}\\
&=\left(\int_{|\lambda|>\lambda_{\max}}\left|e^{-t\lambda^2}\hat{\varphi}^{gr}_{0}(\lambda,\mu,\alpha_\varphi)\right|^2 d\lambda\right)^{\frac{1}{2}}\\
&\oplus_{gr}\left(\int_{|\lambda|\le\lambda_{\max}}\left|e^{\lambda^2(T-t)}\left(\hat{\varphi}^{gr}_{\delta,T}(\lambda,\mu,\alpha_\varphi)\ominus_{gr}\hat{\varphi}^{gr}_{T}(\lambda,\mu,\alpha_\varphi)\right)\right|^2 d\lambda\right)^{\frac{1}{2}}\\
&\le\sup_{|\lambda|>\lambda_{\max}}\frac{e^{-t\lambda^2_{\max}}}{(1+\lambda^2)^{\frac{k}{2}}}\left(\int_{|\lambda|>\lambda_{\max}}\left|\hat{\varphi}^{gr}_{0}(\lambda,\mu,\alpha_\varphi)\right|^2 d\lambda\right)^{\frac{1}{2}}\\
&\oplus_{gr}\sup_{|\lambda|\le\lambda_{\max}}e^{\lambda^2(T-t)}\left(\int_{|\lambda|\le\lambda_{\max}}\left|\left(\hat{\varphi}^{gr}_{\delta,T}(\lambda,\mu,\alpha_\varphi)\ominus_{gr}\hat{\varphi}^{gr}_{T}(\lambda,\mu,\alpha_\varphi)\right)\right|^2 d\lambda\right)^{\frac{1}{2}}\\
&\le\frac{e^{-t\ln((\frac{A}{\delta})^{\frac{1}{T}}(\ln\frac{A}{\delta}))^{-\frac{k}{2T}}}}{(\ln((\frac{A}{\delta})^{\frac{1}{T}}(\ln\frac{A}{\delta})^{-\frac{k}{2T}}))^{\frac{k}{2}}}\oplus_{gr}e^{(T-t)\ln((\frac{A}{\delta})^{\frac{1}{T}})}\delta\\
&=(\frac{A}{\delta})^{-\frac{t}{T}}(\ln\frac{A}{\delta})^{\frac{kt}{2T}}A\left(\frac{1}{\frac{1}{T}\ln\frac{A}{\delta}+\ln(\ln\frac{A}{\delta})^{-\frac{k}{2T}}}\right)^{\frac{k}{2}}+(\frac{A}{\delta})^{\frac{T-t}{T}}\delta(\ln\tfrac{A}{\delta})^{-\frac{k}{2}}\\
&=(\frac{A}{\delta})^{-\frac{t}{T}}(\ln\frac{A}{\delta})^{\frac{kt}{2T}}A\left(\frac{\ln\frac{A}{\delta}}{\frac{1}{T}\ln\frac{A}{\delta}+\ln(\ln\frac{A}{\delta})^{-\frac{k}{2T}}}\right)^{\frac{k}{2}}(\ln\frac{A}{\delta})^{\frac{k}{2}}+A^{1-\frac{t}{T}}\delta^{\frac{t}{T}}(\ln\tfrac{A}{\delta})^{-\frac{k}{2}}\\
&=A^{1-\frac{t}{T}}\delta^{\frac{t}{T}}(\ln\tfrac{A}{\delta})^{-\frac{k}{2}}\left(1+\left(\frac{\ln\frac{A}{\delta}}{\frac{1}{T}\ln\frac{A}{\delta}+\ln(\ln\frac{A}{\delta})^{-\frac{k}{2T}}}\right)^{\frac{k}{2}}\right).
\end{aligned}
$$

Therefore, the proof of convergence estimate is completed. □

This theorem shows the error estimation of the Fourier regularization method. When the input data is noisy, the results show that the error between the regularized solution and the exact solution can be effectively controlled within a certain range. When certain conditions are met, with the reduction of the noise level, the regularized solution will converge to the exact solution at a certain rate, which provides a solid theoretical basis for evaluating and optimizing the Fourier regularization method in practical applications.

Remark 4.3. *When $k = 0$, Eq* (4.14) *becomes*

$$
\| u^{gr}(\cdot,t,\mu,\alpha_u)\ominus_{gr}u^{gr}_{\delta,\lambda_{\max}}(\cdot,t,\mu,\alpha_u)\|\le 2A^{1-\frac{t}{T}}\delta^{\frac{t}{T}}. \tag{4.15}
$$

We know this is a *Hölder* error estimate. At $t = 0$, it just means that, with $2A$ as the error bound, you cannot actually tell whether the regular solution is stable at $t = 0$. However, this defect can be

corrected by Eq (4.14). In fact, for $t = 0$, Equation (4.14) becomes

$$\| u^{gr}(\cdot,0) \ominus_{gr} u^{gr}_{\delta,\lambda_{\max}}(\cdot,0) \| \leq A(\ln\frac{A}{\delta})^{-\frac{k}{2}}\left(1+\left(\frac{\ln\frac{A}{\delta}}{\frac{1}{T}\ln\frac{A}{\delta}+\ln(\ln\frac{A}{\delta})^{-\frac{k}{2T}}}\right)^{\frac{k}{2}}\right)\longrightarrow 0, \tag{4.16}$$

as $\delta \longrightarrow 0$ and $k > 0$.

Remark 4.4. *We know that in actual calculation, the prior bound A given by us is unknown. For the convenience of calculation, if we take the prior bound as $A = 1$, then*

$$\lambda_{\max} = \left(\ln\left(\left(\frac{1}{\delta}\right)^{\frac{1}{T}}\left(\ln\frac{1}{\delta}\right)^{-\frac{k}{2T}}\right)\right)^{\frac{1}{2}}, \tag{4.17}$$

and we also have the estimate

$$\| u^{gr}(\cdot,t,\mu,\alpha_u) \ominus_{gr} u^{gr}_{\delta,\lambda_{\max}}(\cdot,t,\mu,\alpha_u) \| \leq \delta^{\frac{t}{T}}(\ln\tfrac{1}{\delta})^{-\frac{k}{2}}\left(1+\left(\frac{\ln\frac{A}{\delta}}{\frac{1}{T}\ln\frac{1}{\delta}+\ln(\ln\frac{1}{\delta})^{-\frac{k}{2T}}}\right)^{\frac{k}{2}}\right). \tag{4.18}$$

5. Numerical example

Example 5.1. *The initial value problem of the following form of the BHCE with uncertainty in an unbounded region is considered:*

$$\begin{cases}\partial_{t_{gr}}\tilde{u}(x,t) \ominus_{gr} \dfrac{1}{4}\partial_{xx_{gr}}\tilde{u}(x,t) = 0, \quad x \in \mathbb{R}; t \in [0,T),\\ \tilde{u}(x,0) = \tilde{v}(x)e^{-x^2},\end{cases} \tag{5.1}$$

where $\tilde{v}(x)$ is a fuzzy-number-valued function, i.e., $\tilde{v}(x) = (-5,0,5)$, and we have the following expression:

$$\tilde{v}(x) = \begin{cases}\dfrac{1}{5}x+1, & x \in [-5,0),\\ 1, & x = 0,\\ -\dfrac{1}{5}x+1, & x \in (0,5],\\ 0, & otherwise,\end{cases} \tag{5.2}$$

and, according to Definition 2.2, $v^{gr}(x,\mu,\alpha_v) = (-5+5\mu)+10(1-\mu)\alpha_v$. Based on Remark 2.11, we obtain the granular differential equation as follows:

$$\begin{cases}\partial_{t_{gr}}u^{gr}(x,t,\mu,\alpha_u) \ominus_{gr} \dfrac{1}{4}\partial_{xx_{gr}}u^{gr}(x,t,\mu,\alpha_u) = 0, & x \in \mathbb{R}; t \in [0,T),\\ u^{gr}(x,0,\mu,\alpha_u) = [(-5+5\mu)+10(1-\mu)\alpha_v]\cdot e^{-x^2}, & \alpha_u = \alpha_v \in [0,1].\end{cases} \tag{5.3}$$

Then, from Eq (2.20)*, the exact solution of Eq* (5.3) *is*

$$u^{*gr}(x,t,\mu,\alpha_u) = [(-5+5\mu)+10(1-\mu)\alpha_v]\cdot\frac{1}{\sqrt{1+t}}e^{-\frac{x^2}{1+t}}, \tag{5.4}$$

and, according to Remark 2.3*, the* μ*-level sets of the exact solution can be obtained as*

$$[\tilde{u}^*(x,t)]_\mu = [-5+5\mu, 5-5\mu]\cdot\frac{1}{\sqrt{1+t}}e^{-\frac{x^2}{1+t}}. \tag{5.5}$$

Therefore, $\tilde{u}^*(x,t)$ *is also a solution to the following fuzzy backward heat conduction equation*

$$\begin{cases} \partial_{t_{gr}}u^{gr}(x,t,\mu,\alpha_u)\ominus_{gr}\dfrac{1}{4}\partial_{xx_{gr}}u^{gr}(x,t,\mu,\alpha_u)=0, & x\in\mathbb{R}; t\in[0,T), \\ u^{gr}(x,T,\mu,\alpha_u)=[(-5+5\mu)+10(1-\mu)\alpha_v]\cdot\dfrac{1}{\sqrt{1+T}}e^{-\frac{x^2}{1+T}}, & \alpha_u=\alpha_v\in[0,1]. \end{cases} \tag{5.6}$$

Numerical experiments will be performed below. Then, according to the Fourier regularization method, the Fourier regular solution of the above Eq (5.6) is constructed as follows:

$$u^{gr}_{\delta,\lambda_{\max}}(x,t,\mu,\alpha_u) = \frac{1}{\sqrt{\pi t}}\int_{-\infty}^{+\infty} e^{-\frac{(x-\lambda)^2}{t}}\hat{\varphi}^{gr}_{\delta,T}(\lambda,\mu,\alpha_\varphi)\zeta_{\max}d\lambda, \tag{5.7}$$

where $\zeta_{\max}$ is the characteristic function of the interval $[-\lambda_{\max},\lambda_{\max}]$, and $\hat{\varphi}^{gr}_{\delta,T}(\lambda,\mu,\alpha_\varphi)$ is the fuzzy Fourier transform of the measurement data $\varphi^{gr}_{\delta,T}(x,\mu,\alpha_\varphi)$ obtained by physical instruments at time $t=T$, which is usually with errors. Noise data is generated by the *rand*$(\cdot)$ function of MATLAB.

$$(\varphi^{gr}_{\delta,T}(x,\mu,\alpha_\varphi))_i = (\varphi^{gr}_T(x,\mu,\alpha_\varphi))_i + \epsilon\cdot rand(size(\varphi^{gr}_T(x,\mu,\alpha_\varphi)))_i, \tag{5.8}$$

where $(\varphi^{gr}_T(x,\mu,\alpha_\varphi))_i$ is the exact data and $rand(size(\varphi^{gr}_T(x,\mu,\alpha_\varphi)))_i$ is a random number of the same dimension as $(\varphi^{gr}_T(x,\mu,\alpha_\varphi))$ on $[0,1]$. The magnitude ϵ indicates the noise level of measurement data by physical instruments, and this noise level has an expression as follows:

$$\epsilon :\triangleq \| \varphi^{gr}_{\delta,T}(\lambda,\mu,\alpha_\varphi) \| = \left(\frac{1}{N_x}\sum_{i=1}^{N_x}|\varphi^{gr}_{\delta,T}(\lambda_i,\mu,\alpha_\varphi)-\varphi^{gr}_T(\lambda_i,\mu,\alpha_\varphi)|^2\right)^{\frac{1}{2}}. \tag{5.9}$$

In this experiment, we mainly used *MATLAB R* 2016*a* for numerical simulation and calculation. Before regularization, we first present the results obtained unregularization. Figures 2 and 3 show the results for noise levels $\epsilon = 6\times10^{-2}$ and $\epsilon = 6\times10^{-4}$, respectively, with $T=1$ and $t=0$.

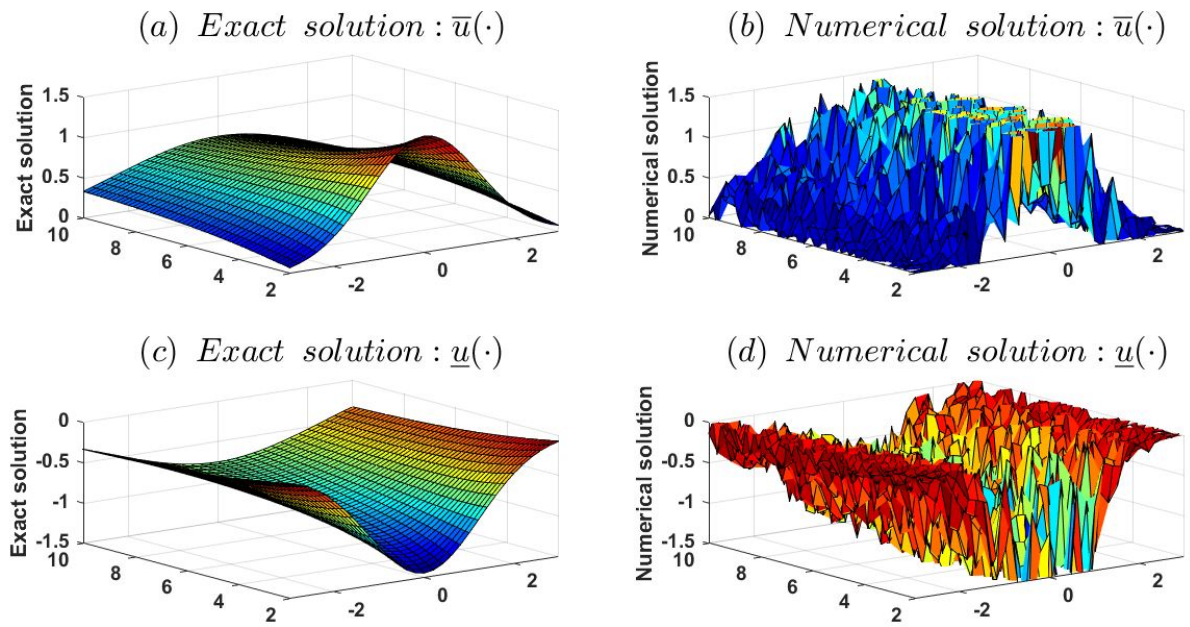

Figure 2. $T = 1, t = 0, \epsilon = 6 \times 10^{-2}$.

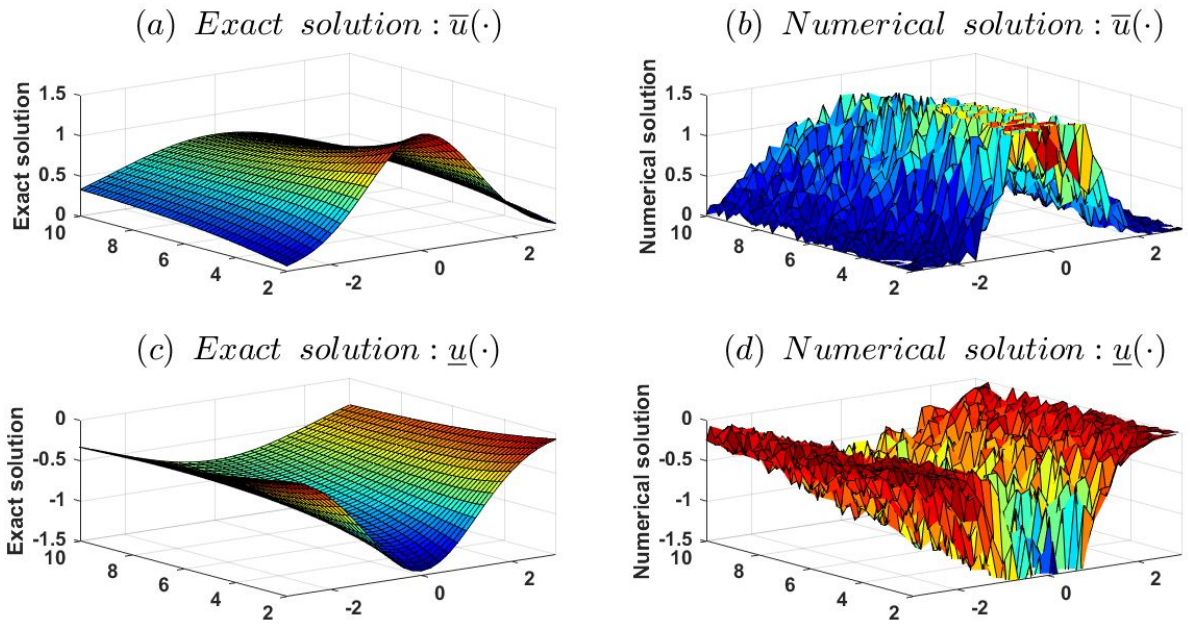

Figure 3. $T = 1, t = 0, \epsilon = 6 \times 10^{-4}$.

It is evident that the higher the noise level, the less accurate the unregularized solution becomes. Therefore, when the input data is not processed through regularization, even minor perturbations in the input data can lead to significant changes in the solution, rendering the numerical solution highly unstable.

Figure 4 show the exact solution of the Eq (5.1), taking $\mu = 0$, 0.25, 0.5, 0.75, and 1, respectively. In these figures, the upper and lower halves of the graph represent the left and right endpoints of the μ-level sets of the exact solution, respectively, and the red curve represents $\mu = 1$.

Figure 5 show the Fourier regular solution of Eq (5.1) obtained by Fourier regularization, taking $\mu = 0, 0.25, 0.5, 0.75$, and 1, respectively. The regularization parameter $\lambda_{\max} = 0.9124$.

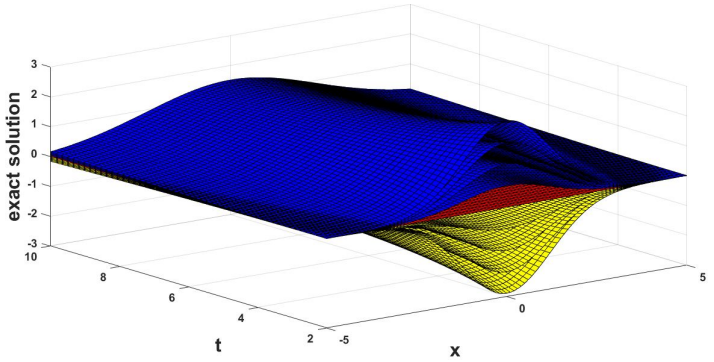

Figure 4. Exact solution.

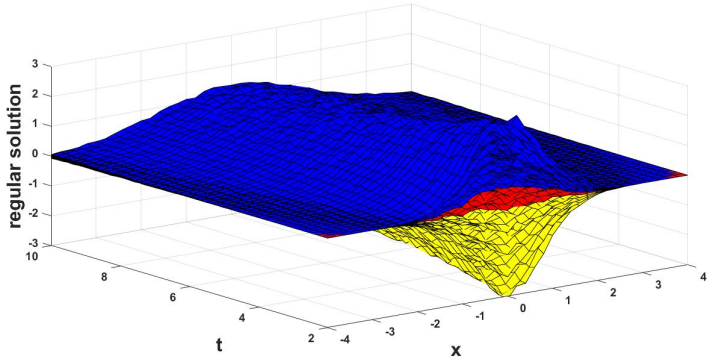

Figure 5. Fourier regular solution, $\lambda_{\max} = 0.9124$.

From Figures 4 and 5, we can clearly see that appropriate selection of regularization parameter values can make regular solutions stably approximate the exact solution. To further investigate this example under the granular differentiability concept, here we take special values $x = 1$ and $t = 1$ to observe the numerical results, i.e., we fix $x = 1$ and $t = 1$, respectively, to observe the relationship between the exact and regular solutions.

Figure 6 shows the exact solution of Eq (5.1) when $x = 1$ is fixed, with μ taking values of 0, 0.25, 0.5, 0.75, and 1, respectively. The blue and red curves show left and right endpoints of the μ-level sets of the exact solution of the Eq (5.1), respectively, and the black curve corresponds to the level $\mu = 1$.

Figure 7 shows that when $x = 1$ is fixed, the Fourier regular solution of Eq (5.1) obtained by Fourier regularization takes $\mu = 0, 0.25, 0.5, 0.75$, and 1, respectively. The regularization parameter $\lambda_{\max} = 0.9124$.

Figure 8 shows that when $t = 1$ is fixed, the exact solution of Eq (5.1) takes values corresponding $\mu = 0, 0.25, 0.5, 0.75$, and 1, respectively.

Figure 9 shows that when $t = 1$ is fixed, the Fourier regular solution of Eq (5.1) obtained by Fourier regularization takes $\mu = 0, 0.25, 0.5, 0.75$, and 1, respectively.

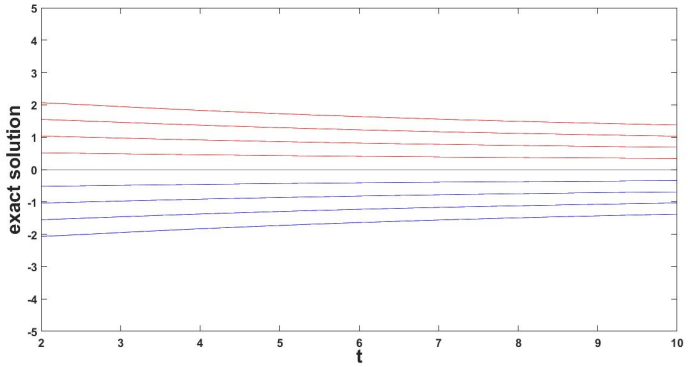

Figure 6. Fixed $x = 1$, exact solution.

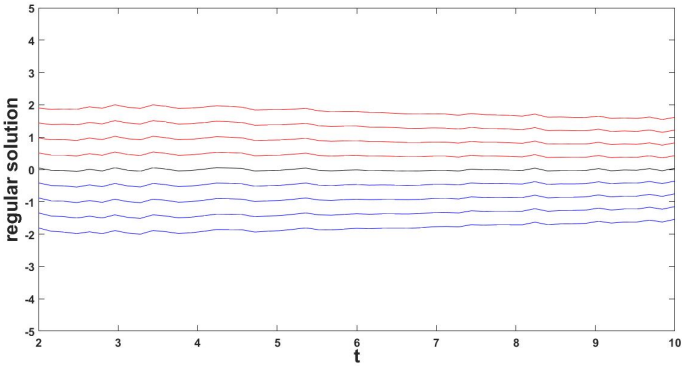

Figure 7. Fixed $x = 1$, Fourier regular solution, $\lambda_{\max} = 0.9124$.

The above numerical experiments are done with noise level $\epsilon = 6 \times 10^{-2}$ on the given data. As can be seen from Figures 8 and 9, Fourier regularization method can stabilize regular solutions to exact solutions well if appropriate regularization parameter values are selected. From the fixed $x = 1$ and $t = 1$, it is not difficult to find that when $\mu = 1$, the solution of the uncertain reverse heat conduction equation obtained by Fourier regularization is completely consistent with the solution in the classical sense.

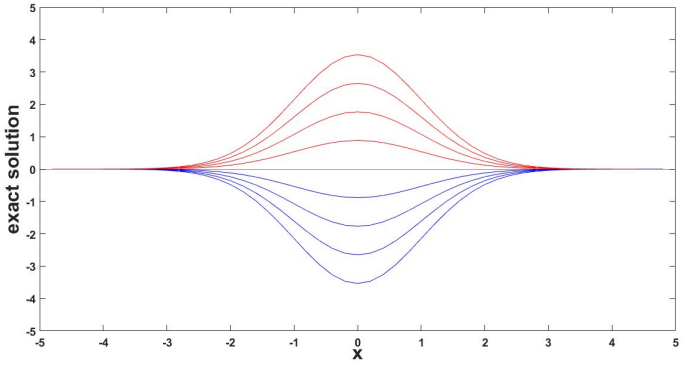

Figure 8. Fixed $t = 1$, exact solution.

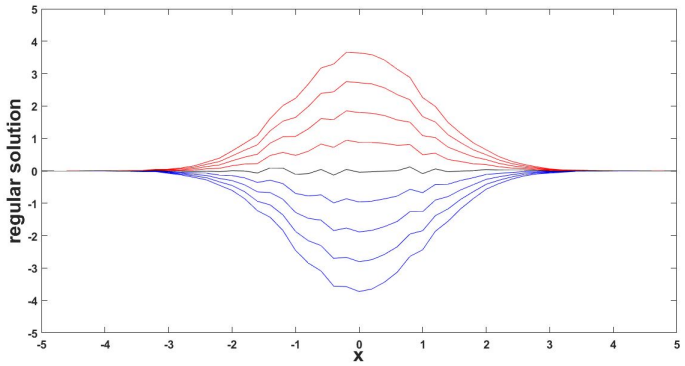

Figure 9. Fixed $t = 1$, Fourier regular solution, $\lambda_{\max} = 0.9124$.

In the following, we illustrate the numerical results of the Fourier regularization method when taking different regularization parameters. The purpose is to prove that the exact solution can be approached well by selecting suitable regularization parameters, and the optimal regularization parameters can also be found by this method. It can also be further explained that the regularization parameter selection scheme we give, that is, Equation (4.13), is very effective.

Figures 10–12 are the results of Fourier regularization with regularization parameter $\lambda_{\max} = 1.1736$ and noise level $\epsilon = 6 \times 10^{-2}$. In Figures 11 and 12, $x = 1$ and $t = 1$ are fixed, respectively. It is obvious that the Fourier regularization results are not optimistic when the regularization parameter values are large.

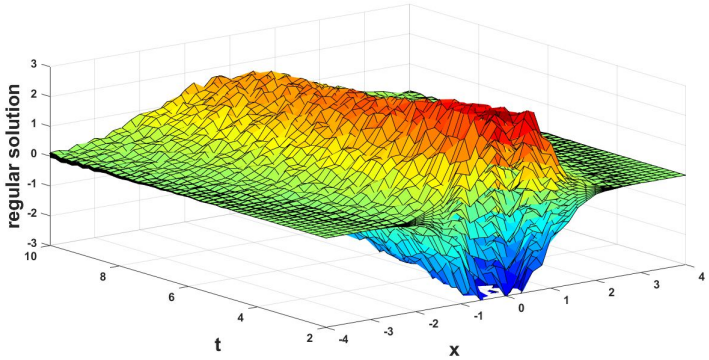

Figure 10. Fourier regular solution, $\lambda_{\max} = 1.17136$; $\epsilon = 6 \times 10^{-2}$.

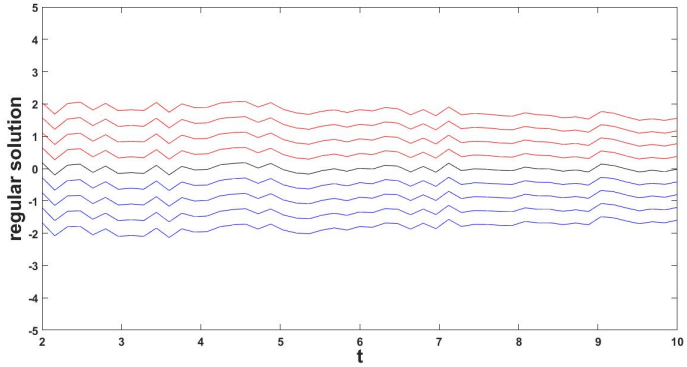

Figure 11. Fixed $x = 1$; Fourier regular solution, $\lambda_{\max} = 1.17136$; $\epsilon = 6 \times 10^{-2}$.

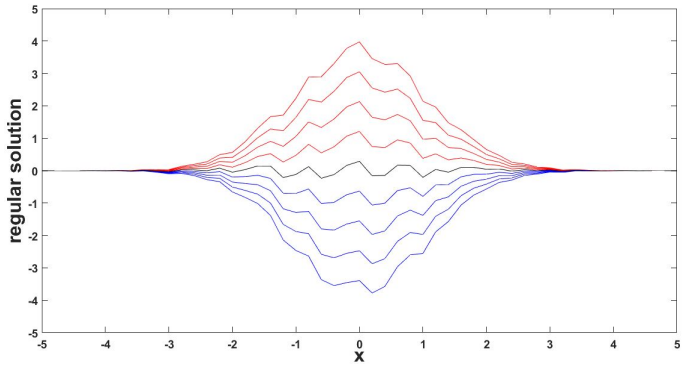

Figure 12. Fixed $t = 1$; Fourier regular solution, $\lambda_{\max} = 1.17136$; $\epsilon = 6 \times 10^{-2}$.

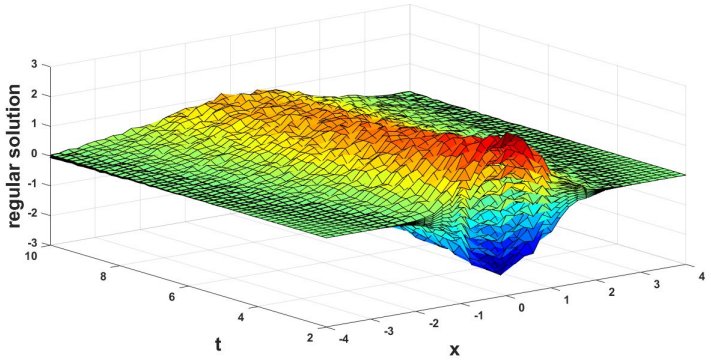

Figure 13. Fourier regular solution, $\lambda_{\max} = 0.5697$; $\epsilon = 6 \times 10^{-2}$.

Figures 13–15 are the results of Fourier regularization when the regularization parameter $\lambda_{\max} = 0.5697$ and the noise level $\epsilon = 6 \times 10^{-2}$. In Figures 14 and 15, $x = 1$ and $t = 1$ are fixed, respectively. It is obvious that Fourier regularization results are not optimistic when the regularization parameter values are small.

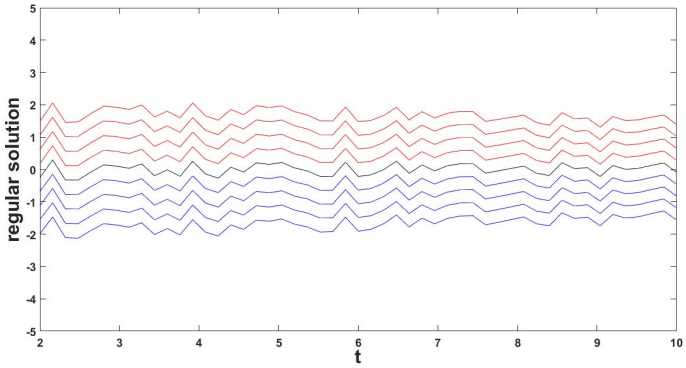

Figure 14. Fixed $x = 1$; Fourier regular solution, $\lambda_{\max} = 0.5697$; $\epsilon = 6 \times 10^{-2}$.

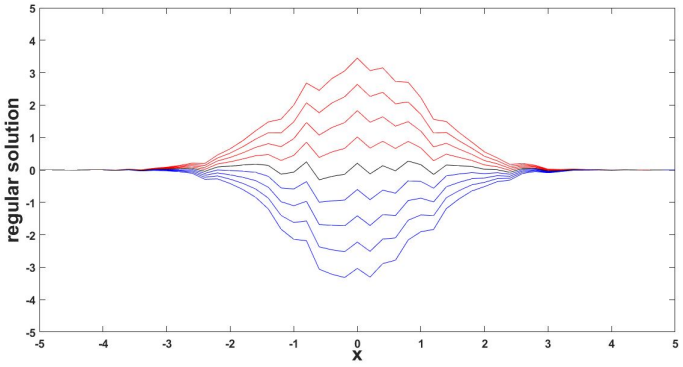

Figure 15. Fixed $t = 1$; Fourier regular solution, $\lambda_{\max} = 0.5697$; $\epsilon = 6 \times 10^{-2}$.

We can see from the graph above that if the regularization parameter value is large or small, there will be a large error between the regular solution and the exact solution. Therefore, choosing the appropriate regularization parameter value is the key to solving this kind of problem. According to the selection scheme of regularization parameters given in this paper, the regular solution can well approach the exact solution. In this example, we can also observe that when $\mu = 1$, the solution of the BHCE with uncertainty is the solution of the BHCE in the classical sense.

This not only shows the validity of our method, but also provides a new solution for solving the inverse problem of the uncertainty equation. Compared with the deterministic equation, the solution of the uncertain equation is an interval, which increases the control range and can improve the precision accordingly.

Through the above analysis, it can be seen that the regularization parameter rule given by Eq (4.13) is valid. For this example, when the value of the regularization parameter is 0.9124, the regular solution and the exact solution have the best stability. The figure below shows that the numerical solution of the proposed method is stable at $t = 0$. This is consistent with our theoretical results.

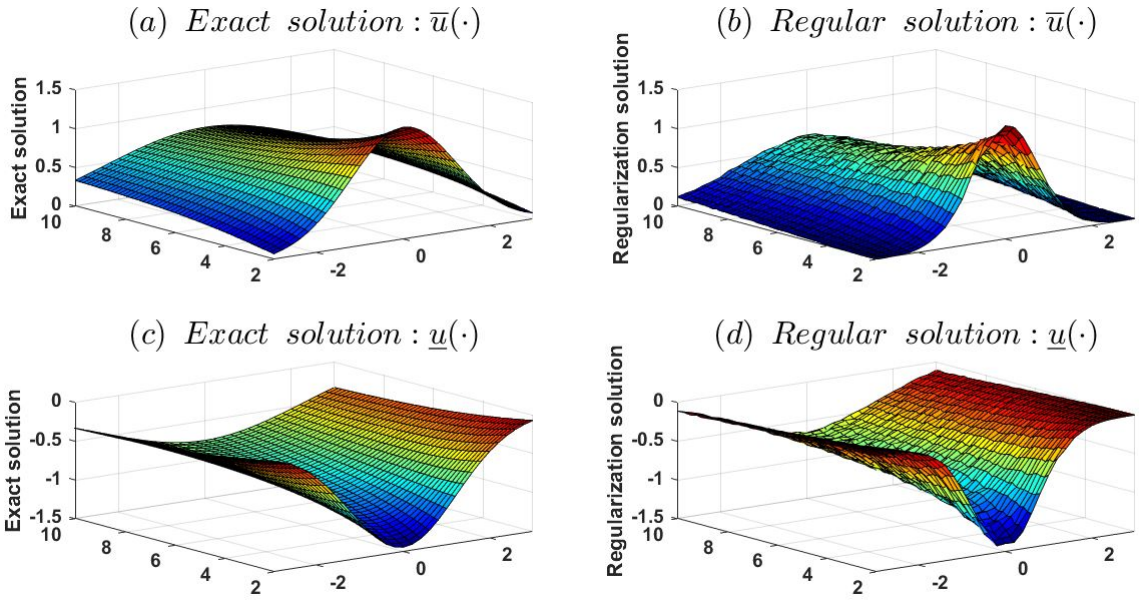

Figure 16. Stability of the regular solution at $t = 0$.

We already know that, the higher the value of T, the flatter the exact solution. Therefore, as the T-value increases, we also adjust the regularization parameters accordingly, so that the regular solution is stabilizes well to the exact solution. The following two figures show the regularization results for $T = 10$ and $T = 100$, respectively. It can be seen that Fourier regularization yields satisfactory results in these cases.

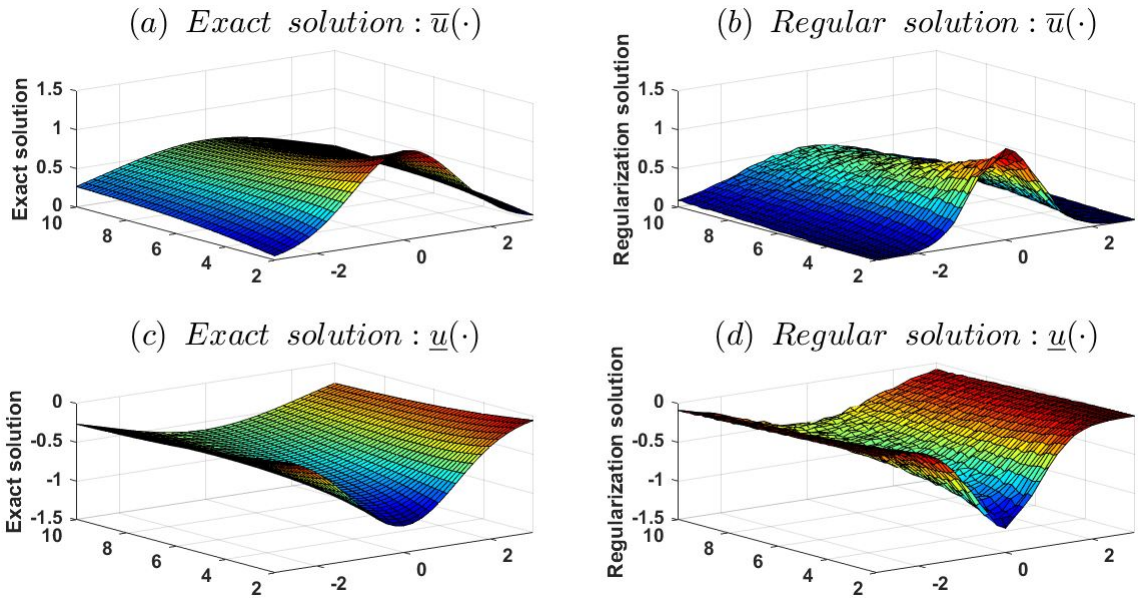

Figure 17. $T = 10$, $\lambda_{\max} = 0.9583$, $\epsilon = 6 \times 10^{-2}$.

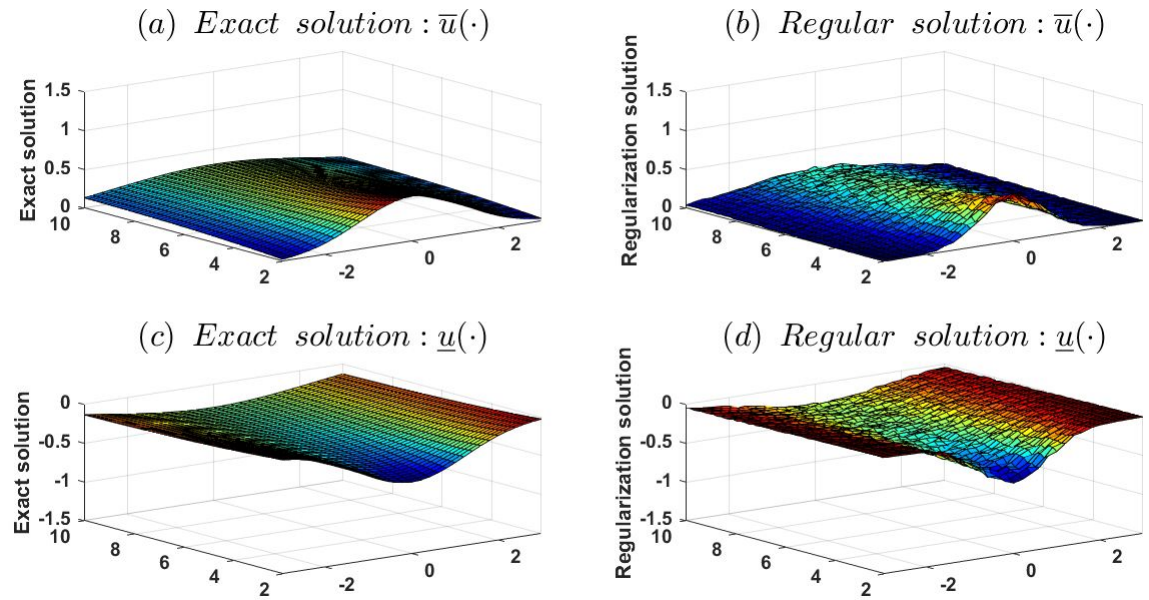

Figure 18. $T = 100$, $\lambda_{\max} = 0.9583$, $\epsilon = 6 \times 10^{-2}$.

Through the analysis of the above example, even if there is noise in the given data, we can make it tend to a stable solution through the Fourier regularization method. This numerical example also

further verifies the effectiveness and practicability of the Fourier regularization method proposed in this paper.

The following example shows that Fourier regularization is still valid under different fuzzy initial conditions.

Example 5.2. *We consider the following BHCE with uncertainty:*

$$\begin{cases} \partial_{t_{gr}}\tilde{u}(x,t) \ominus_{gr} \dfrac{1}{4}\partial_{xx_{gr}}\tilde{u}(x,t) = 0, \quad x \in \mathbb{R}; t \in [0,T), \\ \tilde{u}(x,0) = \tilde{v}(x) \cdot \sin x, \end{cases} \tag{5.10}$$

where $\tilde{v}(x) = (-1, 0, 1)$ *is a fuzzy-number-valued function, and, according to Definition* 2.2*, we have* $v^{gr}(x, \mu, \alpha_v) = (\mu - 1) + 2(1 - \mu)\alpha_u$*. Based on Remark* 2.11*, we obtain the granular differential equation as follows:*

$$\begin{cases} \partial_{t_{gr}}u^{gr}(x,t,\mu,\alpha_u) \ominus_{gr} \dfrac{1}{4}\partial_{xx_{gr}}u^{gr}(x,t,\mu,\alpha_u) = 0, \quad x \in \mathbb{R}; t \in [0,T), \\ u^{gr}(x,0,\mu,\alpha_u) = [(\mu-1) + 2(1-\mu)\alpha_v] \cdot \sin x, \quad \alpha_u = \alpha_v \in [0,1]. \end{cases} \tag{5.11}$$

The exact solution of Eq (5.11) *is*

$$u^{*gr}(x,t,\mu,\alpha_u) = [(\mu-1) + 2(1-\mu)\alpha_v] \cdot e^{-t} \sin x, \tag{5.12}$$

and according to Remark 2.3*, the* μ*-level sets of the exact solution can be obtained:*

$$[\tilde{u}^*(x,t)]_\mu = [\mu - 1, 1 - \mu] \cdot e^{-t} \sin x. \tag{5.13}$$

Therefore, $\tilde{u}^*(x,t)$ *is also a solution to the following fuzzy backward heat conduction equation:*

$$\begin{cases} \partial_{t_{gr}}u^{gr}(x,t,\mu,\alpha_u) \ominus_{gr} \dfrac{1}{4}\partial_{xx_{gr}}u^{gr}(x,t,\mu,\alpha_u) = 0, \quad x \in \mathbb{R}; t \in [0,T), \\ u^{gr}(x,T,\mu,\alpha_u) = [\mu-1) + 2(1-\mu)\alpha_v] \cdot e^{-T} \sin x, \quad \alpha_u = \alpha_v \in [0,1]. \end{cases} \tag{5.14}$$

In the following experiment, we also tested under the software *MATLAB R* 2016*a*. Here, the noise data is generated in the same way as in the previous example. Our main purpose here is to study the accuracy of regularization methods under different fuzzy initial conditions.

Figures 19 and 20 are the result of the unregularization of this example when $T = 1$, and the noise levels $\epsilon = 6 \times 10^{-2}$ and $\epsilon = 6 \times 10^{-4}$ are taken, respectively.

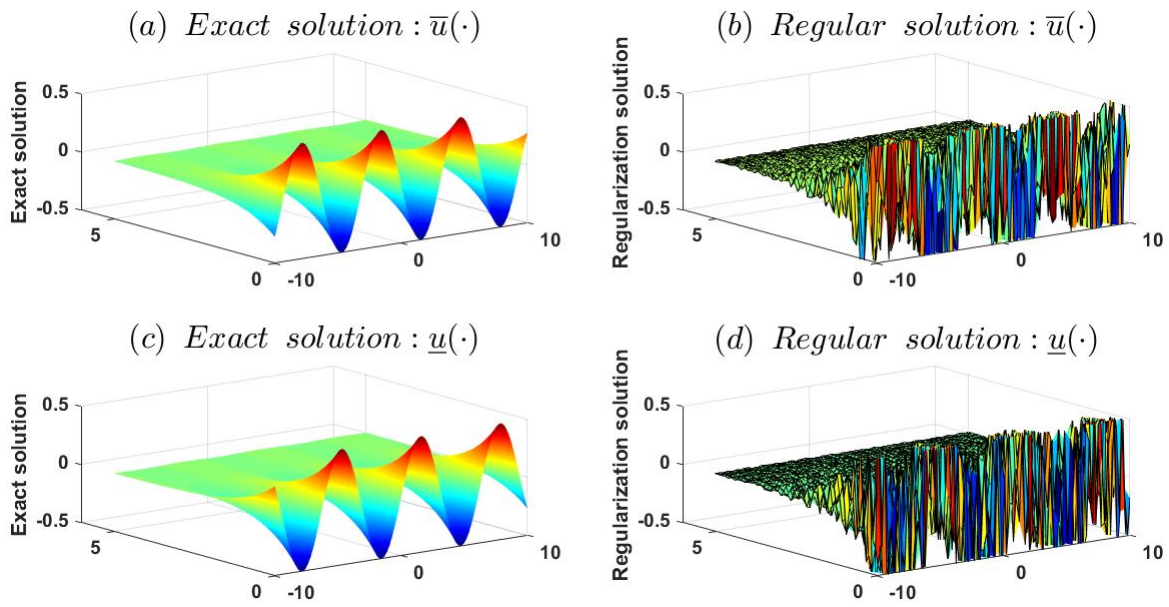

Figure 19. $T = 1$, $t = 0$, $\epsilon = 6 \times 10^{-2}$.

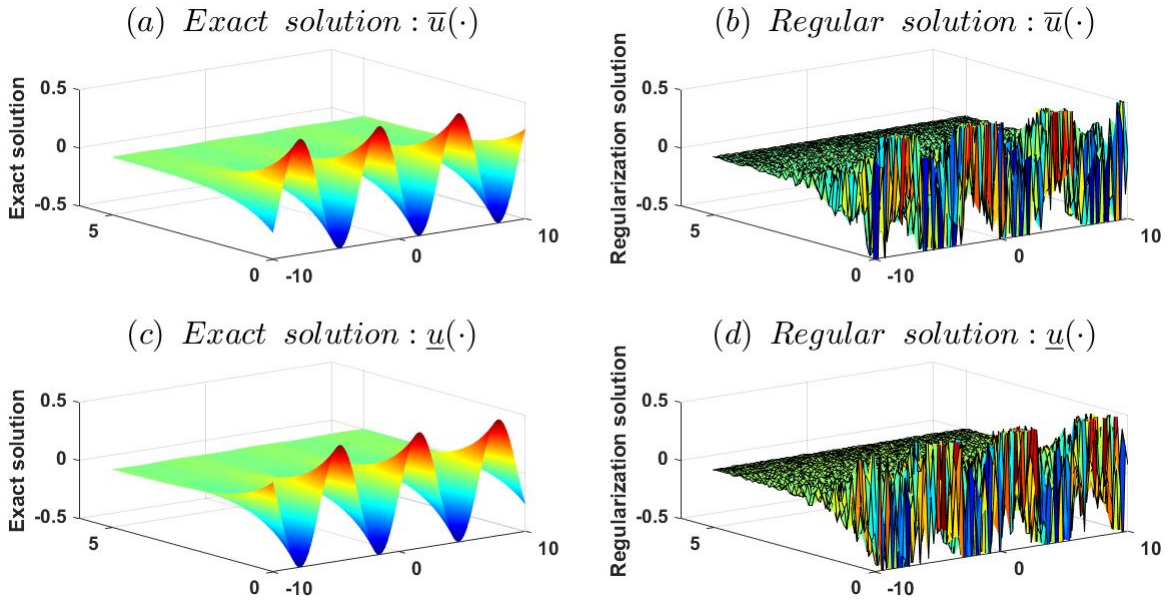

Figure 20. $T = 1$, $t = 0$, $\epsilon = 6 \times 10^{-4}$.

As can be seen from Figures 19 and 20, in the case of unregularization, small perturbations in the input data will cause huge changes in the solution, and this problem is seriously ill-posed. Next, we apply the regularization method to stabilize the numerical solution.

For this example, we calculated the regularization parameters applicable to this example according to the regularization parameter selection scheme, namely Eq (4.13), and compared the difference between the obtained regularization solution and the exact solution of the equation so as to test the stability of the proposed regularization method.

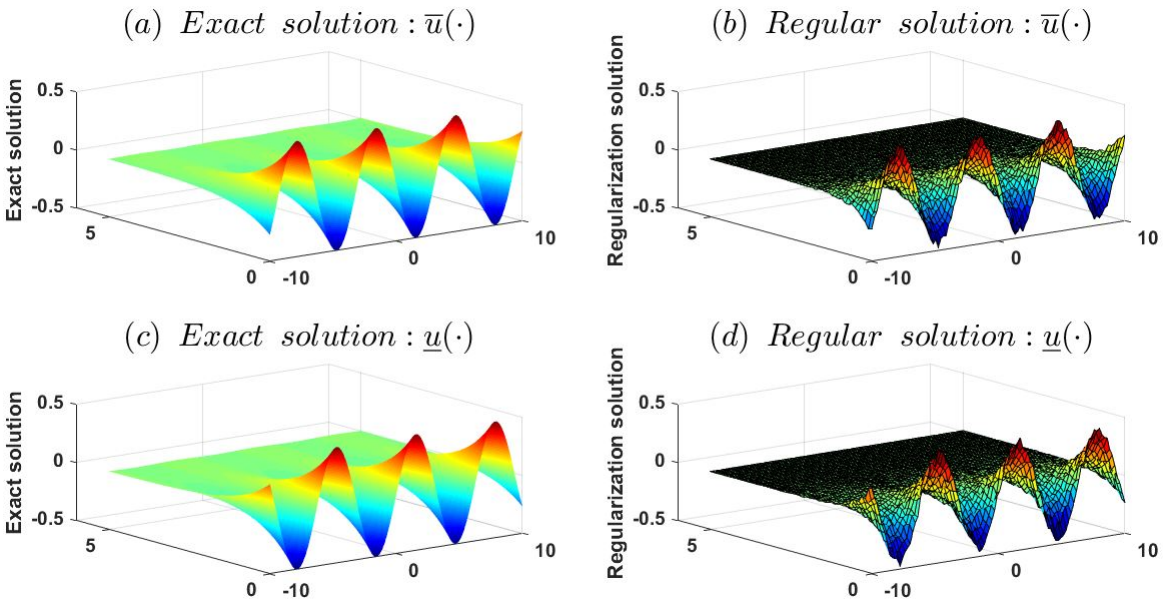

Figure 21. $T = 1$, $\lambda_{\max} = 0.9124$, $\epsilon = 6 \times 10^{-2}$.

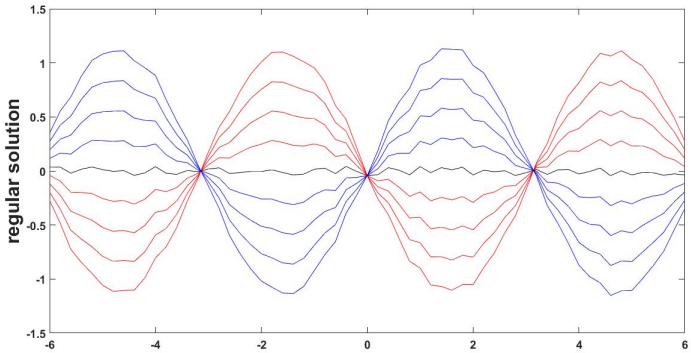

Figure 22. Fixed $t = 1$, $\lambda_{\max} = 0.9124$, $\epsilon = 6 \times 10^{-2}$.

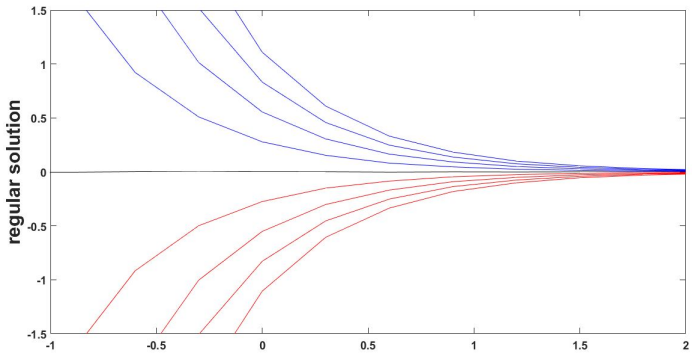

Figure 23. Fixed $x = 1$, $\lambda_{\max} = 0.9124$, $\epsilon = 6 \times 10^{-2}$.

Figure 21 is the result of Fourier regularization. With regularization parameter $\lambda_{\max} = 0.9124$, it can be seen that the regular solution is effectively stable to the exact solution.

Next, we will discuss the stability of the regularization method when fixing $x = 1$ and $t = 1$, respectively.

Figures 22 and 23 show the interval solution plots for fixed $t = 1$ and $x = 1$, respectively, in this example.

It can be seen from the figure that the interval solution obtained by Fourier regularization method is stable even if $t = 1$ and $x = 1$ are fixed.

Next, we take $T = 10$ and $T = 100$ respectively to observe the stability of Fourier regularization method.

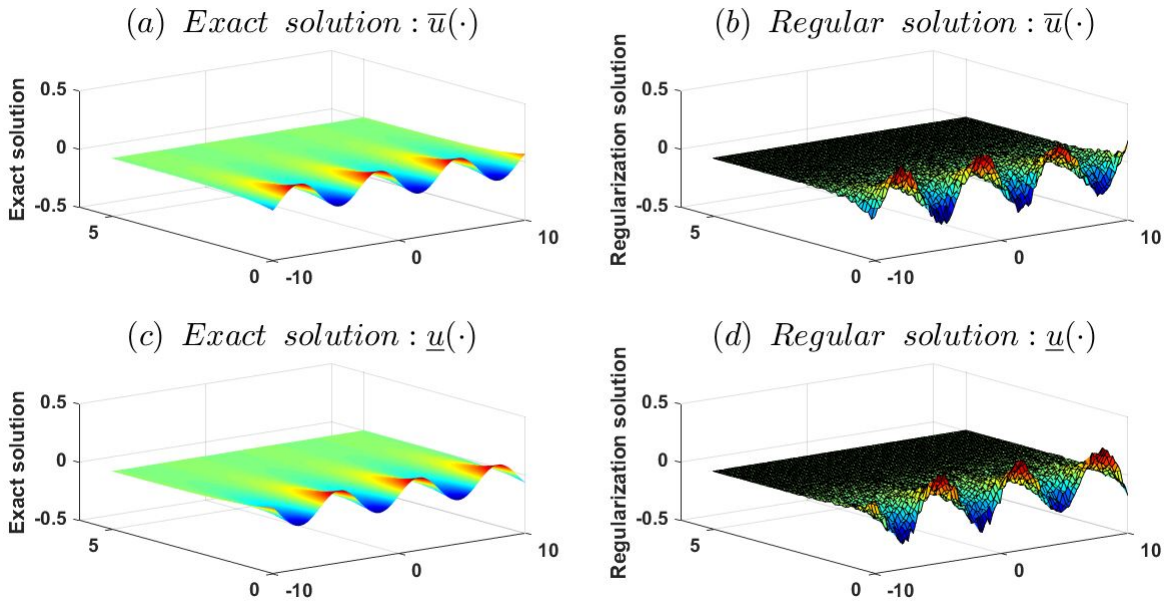

Figure 24. $T = 10$, $\lambda_{\max} = 0.9583$, $\epsilon = 6 \times 10^{-2}$.

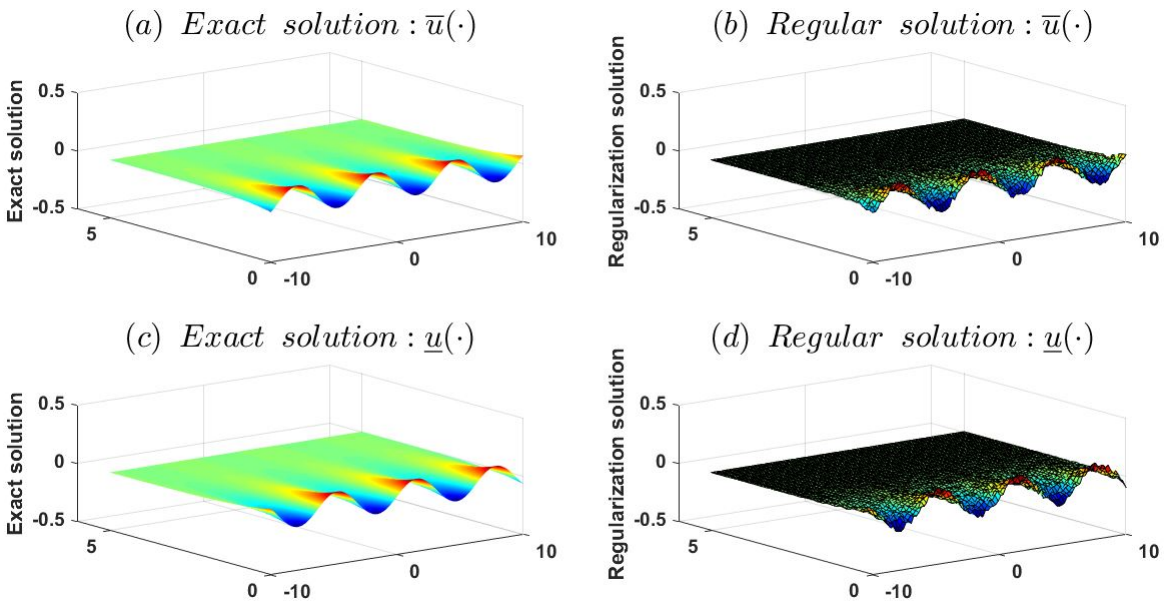

Figure 25. $T = 100$, $\lambda_{\max} = 0.9583$, $\epsilon = 6 \times 10^{-2}$.

From the above example, we can observe that small perturbations in the data can cause large changes in the solution. Fourier regularization method is used to stabilize the numerical solution. By fixing the graph of $t = 1$ and $x = 1$, respectively, it is not difficult to find that when $\mu = 1$, the result obtained is consistent with the result in the classical sense.

The calculation of the above numerical examples were performed using the MATLAB software. Given the small scale of the problem, the limited amount of data, and the high efficiency of the algorithm employed, the computational time for these examples is very brief, typically taking only a few seconds to complete. Specifically, using MATLAB's built-in timer function, we measured the computational time to be approximately 1.2 seconds. This further demonstrates the efficiency and applicability of our algorithm.

6. Conclusions and prospects

In this study, we propose the backward heat conduction equation (BHCE) with uncertainty, in which the uncertainty of parameters is expressed by fuzzy numbers. This equation is essentially an inverse fuzzy differential equation, and we study its numerical solution. Second, it is proved that the backward heat conduction equation (BHCE) with uncertainty is a seriously ill-posed problem, so a specific regularization method is needed to solve its numerical solution. Last, the Fourier regularization method under the granular differentiability concept is used to solve the numerical solution. The granular representation of the regular solution is given, and the convergence and stability estimations of the method are proved under the prior assumptions of the exact solution.

In numerical examples, we use the $rand(\cdot)$ function in MATLAB to randomly generate numbers in the interval $[0, 1]$ to simulate noise in the given data. In this example, we take the noise level of the data $\epsilon = 6 \times 10^{-2}$. We find that when the regularization parameter $\lambda_{\max}$ is calculated according to Eq (4.13), the approximate effect is significant. We also compare different regularization parameters and find that when the regularization parameter is greater than or less than this value, the error between the exact solution and the regular solution is relatively large. At the same time, we also analyze the relationship between the regular solution and the exact solution when $\mu = 0, 0.25, 0.5, 0.75$, and 1 with fixed variables $x = 1$ and $t = 1$, respectively. We find that when $\mu = 1$, the solution of the uncertain BHCE is exactly that of the classical BHCE. This numerical example also shows the practicability and effectiveness of the proposed method.

At present, we define the inverse heat transfer equation based on the granular differentiability concept of fuzzy numerical functions. When uncertainty is represented by fuzzy numbers, the complexity of fuzzy number operation may affect the efficiency of the model. In the future, we can further expand and deepen the definition of fuzzy number differentiability, explore its application in a wider range of mathematical-physical scenarios, and study the properties and solutions of reverse heat conduction equations under different differentiability conditions. Even though we have used the Fourier regularization method, regularization theory is an evolving field. We can explore other types of regularization methods and compare the advantages and disadvantages of different methods in dealing with uncertain reverse heat conduction equations. In practical engineering, the heat conduction process is often coupled with other physical processes. In the future, our method could be extended to the inverse problems of such multi-physical coupling to study its effectiveness in complex practical scenarios. We can apply this method to the field of real-time monitoring and control, such as real-

time monitoring of the heat conduction state and feedback control in the industrial production process. Moreover, we can study how to optimize the method to meet the real-time requirements and enhance its practicality in real-world applications.

Use of AI tools declaration

The authors declare they have not used Artificial Intelligence (AI) tools in the creation of this article.

Acknowledgments

This work is supported by National Natural Science Foundation of China (NO. 12161082) and Gansu Province Outstanding Youth Fund project (Grant No. 24JRRA121). The authors are very grateful to the anonymous referees for their valuable suggestions.

Conflict of interest

The authors declare that they have no conflict of interest.

References

1. J. B. Keller, Inverse problems, *Am. Math. Mon.*, **2** (1976), 107–118. https://doi.org/10.2307/2976988
2. J. Hadamard, *Lecture on Cauchy Problems in Linear Partial Differential Equations*, Yale University Press, New Haven, 1923.
3. A. E. Abouelregal, R. A. Alharb, M. Yaylaci, B. O. Mohamed, S. F. Megahid, Analysis of temperature changes in living tissue using the modified fractional thermal conduction model under laser heat flux on the skin surface, *Continuum Mech. Thermodyn.*, **37** (2025), 1011–1014. https://doi.org/10.1007/s00161-024-01343-y
4. E. A. N. Al-Lehaibi, H. M. Youssef, The heat transfer in skin tissues under the general two-temperature three-phase-lag model of heat conduction with a comparative study, *Heliyon*, **10** (2024), 40257. https://doi.org/10.1016/j.heliyon.2024.e40257
5. L. Liu, C. Liu, Q. M. Zhu, Y. H. Li, Inversion of spatio-temporal distribution heat flux and reconstruction of transient temperature field of three-layered skin tissue during hyperthermia, *J. Therm. Biol.*, **114** (2023), 103515. https://doi.org/10.1016/j.jtherbio.2023.103515
6. A. Carasso, Error bounds in the final value problem for the heat equation, *SIAM J. Math. Anal.*, **7** (1976), 195–199. https://doi.org/10.1137/0507015
7. V. Isakov, *Inverse Problems for Partial Differenticl Equations*, Springer-Verlag, New York, 1998. https://doi.org/10.1007/978-3-319-51658-5
8. W. B. Muniz, H. F. de Campos Veiho, F. M. Ramos, A comparison of some inverse methods for estimating the initial condition of the heat equation, *J. Comput. Appl. Math.*, **103** (1999), 145–163. https://doi.org/10.1016/S0377-0427(98)00249-0

9. W. B. Muniz, F. M. Ramos, H. F. de Campos Veiho, Entropy- and Tihonov-based regularization techniques applied to the backward heat equation, *Int. J. Comput. Math.*, **40** (2000), 1071–1084. https://doi.org/10.1016/S0898-1221(00)85017-8
10. W. Cheng, C. L. Fu, A modified Tikhonov regularization method for an axisymmetric backward heat equation, *Acta Math. Sin. Engl. Ser.*, **26** (2010), 2157–2164. https://doi.org/10.1007/s10114-010-8509-5
11. J. R. Chang, C. S. Liu, C. W. Chang, A new shooting method for quasi-boundary regularization of backward heat conduction problems, *Int. J. Heat Mass Transfer*, **50** (2007), 2325–2332. https://doi.org/10.1016/j.ijheatmasstransfer.2006.10.050
12. S. M. Kirkup, M. Wadsworth, Solution of inverse diffusion problems by operator-splitting methods, *Appl. Math. Model.*, **26** (2002), 1003–1018. https://doi.org/10.1016/S0307-904X(02)00053-7
13. G. Adomian, A review of the decomposition method in applied mathematics, *J. Math. Anal. Appl.*, **135** (1988), 501–544. https://doi.org/10.1016/0022-247X(88)90170-9
14. R. Grzymkowski, M. Pleszczynski, D. Slota, Comparing the Adomian decomposition method and Runge-Kutta method for the solutions of the Stefan problem, *Int. J. Comput. Math.*, **83** (2006), 409–417. http://doi.org/10.1080/00207160600961729
15. M. J. Li, Z. J. Fu, W. Z. Xu, C. M. Fan, A novel spatial-temporal radial Trefftz collocation method for the backward heat conduction analysis with time-dependent source term, *Int. J. Heat Mass Transfer*, **201** (2023), 123627. https://doi.org/10.1016/j.ijheatmasstransfer.2022.123627
16. C. L. Fu, X. T. Xiong, P. Fu, Fourier regularization method for solving the surface heat flux from interior observations, *Math. Comput. Modell.*, **42** (2005), 489–498. https://doi.org/10.1016/j.mcm.2005.08.003
17. C. L. Fu, Simplified Tikhonov and Fourier regularization methods on a general equation, *J. Comput. Appl. Math.*, **167** (2004), 449–463. https://doi.org/10.1016/j.cam.2003.10.011
18. Z. Qian, C. L. Fu, X. T. Xiong, T. Wei, Fourier truncation method for high order numerical derivatives, *Appl. Math. Comput.*, **181** (2006), 940–948. https://doi.org/10.1016/j.amc.2006.01.057
19. C. L. Fu, Y. X. Fu, H. Cheng, Y. J. Ma, The a posteriori Fourier method for solving ill-posed problem, *Inverse Probl.*, **28** (2012), 095002. https://doi.org/10.1088/0266-5611/28/9/095002
20. C. L. Fu, X. L. Feng, Z. Qian, The Fourier regularization for solving Cauchy problem for the Helmholtz equation, *Appl. Numer. Math.*, **59** (2009), 2625–2640. https://doi.org/10.1016/j.apnum.2009.05.014
21. Y. X. Zhang, C. L. Fu, Z. L. Deng, An a posteriori truncation method for some Cauchy problems associated with Helmholtz-type equations, *Inverse Probl. Sci. Eng.*, **21** (2013), 1151–1168. https://doi.org/10.1080/17415977.2012.743538
22. F. Yang, P. Zhang, X. X. Li, The truncation method for the Cauchy problem of the inhomogeneous Helmholtz equation, *Appl. Anal.*, **4** (2017), 991–1004. https://doi.org/10.1080/00036811.2017.1408080

23. J. Kokila, M. T. Nair, Fourier truncation method for the non-homogeneous time fractional backward heat conduction problem, *Inverse Probl. Sci. Eng.*, **28** (2020), 402–426. https://doi.org/10.1080/17415977.2019.1580707
24. S. Y. Duan, B. T. Yang, Determination of singular value truncation threshold for regularization in ill-posed problems, *Inverse Probl. Sci. Eng.*, **8** (2020), 1127–1157. https://doi.org/10.1080/17415977.2020.1832090
25. V. N. Doan, H. T. Nguyen, V. A. Khoa, V. A. Vo, A note on the derivation of filter regularization operators for nonlinear evolution equations, *Appl. Anal.*, **97** (2016), 3–12. https://doi.org/10.1080/00036811.2016.1276176
26. F. Andrzej, W. Agnieszka, C. Michal, Trefftz numerical functions for solving inverse heat conduction problems, *Int. J. Therm. Sci.*, **177** (2022), 107566. https://doi.org/10.1016/j.ijthermalsci.2022.107566
27. M. Ahsan, W. Lei, M. Ahmad, M. S. Hussein, Z. Uddin, A wavelet-based collocation technique to find the discontinuous heat source in inverse heat conduction problems, *Phys. Scr.*, **97** (2022), 125208. https://doi.org/10.1088/1402-4896/ac9dc6
28. D. N. Hao, T. T. Le, L. H. Nguyen, The Fourier-based dimensional reduction method for solving a nonlinear inverse heat conduction problem with limited boundary data, *Commun. Nonlinear Sci. Numer. Simul.*, **128** (2024), 107679. https://doi.org/10.1016/j.cnsns.2023.107679
29. Y. Wang, Z. Qian, Regularizing a two-dimensional time-fractional inverse heat conduction problem by a fractional Landweber iteration method, *Comput. Math. Appl.*, **164** (2024), 104–115. https://doi.org/10.1016/j.camwa.2024.04.001
30. Y. Wang, Z. Qian, A quasi-reversibility method for solving a two-dimensional time-fractional inverse heat conduction problem, *Math. Comput. Simul.*, **212** (2023), 423–440. https://doi.org/10.1016/j.matcom.2023.05.012
31. L. A. Zadeh, Fuzzy sets, *Inf. Control*, **8** (1965), 338–353. https://doi.org/10.1016/S0019-9958(65)90241-X
32. S. S. L. Chang, L. A. Zadeh, On fuzzy mapping and control, *IEEE Trans. Syst. Man Cybern.*, **2** (1972), 30–34. https://doi.org/10.1109/TSMC.1972.5408553
33. D. Dubois, H. Prade, Towards fuzzy differential calculus part 1: Integration of fuzzy mappings, *Fuzzy Sets Syst.*, **8** (1982), 1–17. https://doi.org/10.1016/0165-0114(82)90025-2
34. O. Kaleva, The cauchy problem for fuzzy differential equations, *Fuzzy Sets Syst.*, **35** (1990), 389–396. https://doi.org/10.1016/0165-0114(90)90010-4
35. S. Seikkala, On the fuzzy initial value problem, *Fuzzy Sets Syst.*, **24** (1987), 319–330. https://doi.org/10.1016/0165-0114(87)90030-3
36. B. Bede, Note on "Numerical solutions of fuzzy differential equations by predictor-corrector method", *Inf. Sci.*, **178** (2008), 1917–1922. https://doi.org/10.1016/j.ins.2007.11.016
37. N. Mikaeilvand, S. Khakrangin, Solving fuzzy partial differential equations by fuzzy two-dimensional differential transform method, *Neural Comput. Appl.*, **21** (2012), 307–312. https://doi.org/10.1007/s00521-012-0901-x

38. M. S. Cecconello, R. C. Bassanezi, A. J. V. Brandao, J. Leite, On the stability of fuzzy dynamical systems, *Fuzzy Sets Syst.*, **248** (2014), 106–121. https://doi.org/10.1016/j.fss.2013.12.009

39. M. S. Cecconello, J. Leite, R. C. Bassanezi, A. J. V. Brandao, Invariant and attractor sets for fuzzy dynamical systems, *Fuzzy Sets Syst.*, **265** (2015), 99–109. https://doi.org/10.1016/j.fss.2014.07.017

40. S. Abbasbandy, J. Nieto, M. Alavi, Tuning of reachable set in one dimensional fuzzy differential inclusions, *Chaos Solitons Fractals*, **26** (2005), 1337–1341. https://doi.org/10.1016/j.chaos.2005.03.018

41. M. Chen, Y. Fu, X. Xue, C. Wu, Two-point boundary value problems of undamped uncertain dynamical systems, *Fuzzy Sets Syst.*, **159** (2008), 2077–2089. https://doi.org/10.1016/j.fss.2008.03.006

42. R. Agarwal, V. Lakshmikantham, J. Nieto, On the concept of solution for fractional differential equations with uncertainty, *Nonlinear Anal.*, **72** (2010), 2859–2862. https://doi.org/10.1016/j.na.2009.11.029

43. L. A. Zadeh, Toward a theory of fuzzy information granulation and its centrality in human reasoning and fuzzy logic, *Fuzzy Sets Syst.*, **90** (1997), 111–127. https://doi.org/10.1016/S0165-0114(97)00077-8

44. M. Mazandarani, N. Pariz, A. V. Kamyad, Granular differentiability of fuzzy-number-valued functions, *IEEE Trans Fuzzy Syst.*, **26** (2018), 310–323. https://doi.org/10.1109/TFUZZ.2017.2659731

45. Z. T. Gong, H. Yang, Ill-posed fuzzy initial-boundary value problems based on generalized differentiability and regularization, *Fuzzy Sets Syst.*, **295** (2016), 99–113. https://doi.org/10.1016/j.fss.2015.04.016

46. H. Yang, Z. T. Gong, Ill-posedness for fuzzy Fredholm integral equation of the first kind and regularization methods, *Fuzzy Sets Syst.*, **358** (2019), 132–149. https://doi.org/10.1016/j.fss.2018.05.010

47. H. Yang, Z. T. Gong, Numerical solutions for fuzzy Fredholm inregral equations of the first kind using Landweber iterative method, *J. Intell. Fuzzy Syst.*, **38** (2020), 3059–3074. https://doi.org/10.3233/JIFS-190972

48. O. Kaleva, Fuzzy differential equations, *Fuzzy Sets Syst.*, **24** (1987), 301–317. https://doi.org/10.1016/0165-0114(87)90029-7

49. H. Yang, F. Wang, L. N. Wang, Solving the homogeneous BVP of second order linear FDEs with fuzzy parameters under granular differentiability concept, *J. Intell. Fuzzy Syst.*, **22** (2023), 6327–6340. https://doi.org/10.3233/JIFS-223003

50. Z. Gouyandeh, T. Allahviranloo, S. Abbasbandy, A. Armand, A fuzzy solution of heat equation under generalized Hukuhara differentiability by fuzzy Fourier transform, *Fuzzy Sets Syst.*, **309** (2017), 81–97. https://doi.org/10.1016/j.fss.2016.04.010

51. H. Yang, Y. Chen, Lyapunov stability of fuzzy dynamical systems based on fuzzy-number-valued function granular differentiability, *Commun. Nonlinear Sci. Numer. Simul.*, **133** (2024), 107984. https://doi.org/10.1016/j.cnsns.2024.107984

AIMS Press

© 2025 the Author(s), licensee AIMS Press. This is an open access article distributed under the terms of the Creative Commons Attribution License (https://creativecommons.org/licenses/by/4.0)